

A Thesis

entitled

Verification and Validation Method for  
an Acoustic Mode Prediction Code for Turbomachinery Noise

by

Jeffrey Severino

Submitted to the Graduate Faculty as partial fulfillment of the requirements for the  
Masters of Science Degree in Mechanical Engineering

---

Dr. Ray Hixon, Committee Chair

---

Dr. Chinhua Sheng, Committee Member

---

Dr. Soric Cioc, Committee Member

---

Dr. Patricia R. Komuniecki, Dean  
College of Graduate Studies

The University of Toledo

- 2022

Copyright 2022, Jeffrey Severino

This document is copyrighted material. Under copyright law, no parts of this document may be reproduced without the expressed permission of the author.

An Abstract of  
Verification and Validation Method for  
an Acoustic Mode Prediction Code for Turbomachinery Noise

by  
Jeffrey Severino

Submitted to the Graduate Faculty as partial fulfillment of the requirements for the  
Masters of Science Degree in Mechanical Engineering

The University of Toledo  
- 2022

Over the last 20 years, there has been an increase in computational fluid dynamic codes that have made numerical analysis more and more readily available, allowing turbomachine designers to create more novel designs. However, as airport noise limitations become more restrictive over time, reducing aircraft takeoff and landing noise remains a prominent issue in the aviation community. One popular method to reduce aircraft noise is using acoustic liners placed on the walls of the engine inlet and exhaust ducts. These liners are designed to reduce the amplitude of acoustic modes emanating from the bypass fan as they propagate through the engine. The SWIRL code is a frequency-domain linearized Euler equation solver that is designed to predict the effect of acoustic liners on acoustic modes propagating in realistic sheared and swirling mean flows, guiding the design of more efficient liner configurations. The purpose of this study is to validate SWIRL using the Method Of Manufactured Solutions (MMS). This study also investigated the effect of the integration and spatial differencing methods on the convergence for a given Manufactured Solution. In addition, the effect of boundary condition implementation was tested. The improved MMS convergence rates shown for these tests suggest that the revised SWIRL code provides more accurate solutions with less computational effort than the original formulation.

For my friends and family, who have always believed in my potential when I did not believe it myself.

# Acknowledgments

This work is supported by the NASA Advanced Air Transport Technologies (AATT) Project. I would like to thank Edmane Envia of the NASA Glenn Research Center, who is the technical monitor of this work. A very special thanks goes to Dr. Ray Hixon who supervised and guided me through out my course work and Master's Thesis. His rigor and tenacity in his profession has been the model example for an aspiring aeroacoustician. I would like to also thank all of my committee members, Dr. Chunhua Sheng and Dr. Sorin Cioc. Their contributions have been instrumental. Thanks to Dr. Clifford Brown for his programatic insights.

I would also like to thank my focus group peers, Zaid Sabri, Matthew Gibbons , and Gabriel Gutierrez for their patience and support over the years. I wish them the best in all of their endeavours.

# Contents

<b>Abstract</b>	<b>iii</b>
<b>Acknowledgments</b>	<b>v</b>
<b>Contents</b>	<b>vi</b>
<b>List of Tables</b>	<b>x</b>
<b>List of Figures</b>	<b>xi</b>
<b>List of Symbols</b>	<b>xiii</b>
<b>List of Abbreviations</b>	<b>xv</b>
<b>Preface</b>	<b>xvi</b>
<b>1 Introduction</b>	<b>1</b>
1.1 Overview . . . . .	1
1.1.1 Introduction of overall field and basic explanation of this topic (What) . . . . .	1
1.2 Statement of the of the research questions . . . . .	3
1.2.1 What is already known? . . . . .	3
1.2.2 What is missing?/Why is it a problem? . . . . .	4
1.2.3 The goal and significance of the investigation . . . . .	5
1.3 Definition of the terms (if needed) . . . . .	5

1.4	Organization of research (Structure) . . . . .	5
1.5	Research Questions and Hypothesis . . . . .	6
<b>2</b>	<b>Chapter 2: Literature Review</b>	<b>7</b>
2.1	Introduction . . . . .	7
2.1.1	The problem to be addressed and its significance . . . . .	7
2.1.2	Establish reasoning - i.e. point - of - view for reviewing the literature . . . . .	7
2.1.3	Explain the order/sequence of the review . . . . .	9
2.1.4	The theoretical foundation of conceptual framework . . . . .	10
2.1.5	Work by Kousen . . . . .	10
2.2	Golubev and Atassi's work . . . . .	11
2.3	Review of the assessment of the numerical techniques . . . . .	12
2.3.1	The research questions, hypotheses, foreshadowed problems, or conjectures . . . . .	13
2.4	Conclusion . . . . .	14
<b>3</b>	<b>Chapter 3: Methods</b>	<b>16</b>
3.1	Aerodynamic Models . . . . .	16
3.1.1	Steady Models . . . . .	16
3.1.2	Setting up SWIRL's Aerodynamic Model . . . . .	17
3.2	Applying model to various flows . . . . .	19
3.2.1	Axial Shear Flow . . . . .	19
3.3	Accounting for solid body swirl . . . . .	20
3.3.1	Unsteady Models . . . . .	23
3.4	No Flow . . . . .	23
3.4.0.1	Temporal Derivatives . . . . .	25
3.4.0.2	Radial Derivatives . . . . .	26

3.4.0.3	Tangential Derivatives . . . . .	27
3.4.0.4	Axial Derivatives . . . . .	28
3.4.0.5	Hard Wall boundary condition . . . . .	34
3.5	Uniform Flow . . . . .	35
3.6	Annular Duct Axial Wavenumber solution . . . . .	38
<b>4</b>	<b>Chapter 4: Numerical Models</b>	<b>39</b>
4.1	Numerical Integration . . . . .	39
4.2	Introduction . . . . .	39
4.3	Methods . . . . .	41
4.3.1	Theory . . . . .	42
4.3.2	Procedure . . . . .	46
4.3.3	Tanh Summaion Formulation . . . . .	47
4.4	Fairing Functions . . . . .	51
4.5	Setting Boundary Condition Values Using a Fairing Function . . . . .	51
4.5.1	Using $\beta$ as a scaling parameter . . . . .	51
4.5.2	Minimum Boundary Fairing Function . . . . .	53
4.5.3	Max boundary polynomial . . . . .	55
4.5.4	Corrected function . . . . .	55
4.5.5	Symbolic Sanity Checks . . . . .	56
4.5.6	Min boundary derivative polynomial . . . . .	57
4.5.7	Polynomial function, max boundary derivative . . . . .	58
4.5.8	Putting it together . . . . .	60
<b>5</b>	<b>Results and Discusssion</b>	<b>61</b>
5.1	Verification . . . . .	61
5.2	Introduction . . . . .	61
5.2.1	Statement of the received results and their analysis . . . . .	61



5.3	Code Verificaton using the Method of Manufactured Solutions . . . .	61
5.3.0.1	Test Case 1 . . . . .	71
	<b>References</b>	<b>76</b>

# List of Tables

5.1 Table 4.3 data . . . . . 75

# List of Figures

1-1	The evolution of the directivity and the relative levels of sources as a function of engine architecture (a)low bypass-ratio (b) high bypass ratio [1]	3
5-1	The manufactured mean flow test case using a summation of Tangents for $A$ and $M_x$	63
5-2	The manufactured perturbation functions $,v_r$	63
5-3	The manufactured perturbation functions $,v_x$	64
5-4	The manufactured perturbation functions $,v_\theta$	64
5-5	The manufactured perturbation functions $,P$	65
5-6	A comparison of the speed of sound, expected vs actual at the lowest grid to show similarities in solution	65
5-7	A comparison of the speed of sound error at three grid	66
5-8	A comparison of the speed of sound error at three grid	66
5-9	LEE Source Terms	67
5-10	LEE Source Term Error	67
5-11	LEE Source Term Error	68
5-12	LEE Source Term Error	68
5-13	LEE Source Term Error	69
5-14	L2 Norm comparison for the speed of sound integration for the compound trapezoidal rule	69
5-15	ROC for the speed of sound integration for the compound trapezoidal rule	70

5-16 ROC for the LEE using second and fourth order central differencing for the radial derivative . . . . .	70
--	----

# List of Symbols

$A$ .....	mean flow speed of sound
$A_T$ .....	speed of sound at the duct radius
$\tilde{A}$ .....	dimensionless speed of sound, $\frac{A}{A_T}$
$D/Dt$ .....	material derivative, $\partial/\partial t + V \cdot \nabla$
$D_N$ .....	derivative matrix using $N$ points
$\mathbf{e}_x, \mathbf{e}_\theta$ .....	s
$k_x$ .....	perturbation axial wavenumber
$k$ .....	reduced frequency, $\omega r_{max}/A_T$
$m$ .....	number of nodal diameters, i.e. azimuthal mode number
$M_x$ .....	axial Mach number
$M_\theta$ .....	tangential Mach number
$P$ .....	mean pressure
$p'$ .....	perturbation pressure
$r$ .....	radial coordinate
$r_{min}$ .....	hub radius, i.e. minimum radius
$r_{max}$ .....	hub radius, i.e. maximum radius
$\bar{r}$ .....	dimensionless radial coordinate, $r/r_{max}$
$S$ .....	mean entropy
$s'$ .....	perturbation entropy
$t$ .....	time
$\vec{V}$ .....	mean flow velocity vector
$V$ .....	mean flow velocity
$v'$ .....	perturbation flow velocity
$V_x$ .....	axial component of mean flow velocity
$V_\theta$ .....	tangential component of mean flow velocity
$v'_r$ .....	axial component of perturbation velocity
$v'_x$ .....	axial component of perturbation velocity
$v'_\theta$ .....	tangential component of perturbation flow velocity
$v_\phi$ .....	phase velocity, $k/\bar{\gamma}$
$v_g$ .....	group velocity, $dk/d\bar{\gamma}$
$x$ .....	axial coordinate

### *Greek Symbols*

$\bar{\gamma}$ .....	dimensionless axial wavenumber, $k_x r_{max}$
$\Gamma$ .....	free vortex strength
$\bar{\Gamma}$ .....	$\Gamma/(r_T A_T)$
$\delta$ .....	Kronecker delta
$\eta_H$ .....	hub acoustic liner admittance (at $r_{min}$ )
$\eta_T$ .....	tip acoustic liner admittance (at $r_{max}$ )
$\Theta$ .....	circumferential/azimuthal coordinate
$\kappa$ .....	ratio of specific heats
$\kappa_{m\mu}$ .....	modal separation constant
$\lambda$ .....	eigenvalue, $-i\bar{\gamma}$
$\mu$ .....	radial mode index
$\bar{\rho}$ .....	mean density
$\rho'$ .....	perturbation density
$\sigma$ .....	hub-to-tip radius ratio, $r_{min}/r_{max}$
$\Omega$ .....	angular frequency for solid body swirl
$\bar{\Omega}$ .....	$\Omega r_T/A_T$
$\omega$ .....	perturbation angular frequency

# List of Abbreviations

CAA .....	Computational Aeroacoustics
CFD .....	Computational Fluid Dynamics
MMS .....	Method of Manufactured Solutions
TSM .....	Tanh Summation Method
NS .....	Navier-Stokes
RK .....	Runge-Kutta

# Preface



# Chapter 1

## Introduction

### 1.1 Overview

#### 1.1.1 Introduction of overall field and basic explanation of this topic (What)

Aircraft noise is one of the most environmentally detrimental consequences of commercial flight. Studies suggest that exposure to aircraft noise leads to diminished academic performance in youth, and could increase the risk of cardiovascular disease for populations close to airports [2]. Although the COVID-19 pandemic reduced air passenger traffic by 96% between 2019 and 2020, [3] the global aviation community has proven to be resilient during times of economic shock. The International Air Transport Association (IATA) has studied the resilience of the global air passenger markets after four notable shocks to the aviation economy; The impact of four notable events, (1979 oil shock, 2000-2001 dot-com bust, 9/11, and the 2008 financial crisis) was studied by a statistical analysis of the estimated 'passenger gap' from 1950-2014. Data shows that approximately 72% of the impact of the initial shock persists one year after the event and diminishes to just under one-fifth of the initial impact. Given these trends in air transportation, the need for aviation noise regulation persists and

will continue to be a concern so long as the aviation continues this rate of growth.

Since the dawn of commercial airlines in the early 20th century, the increased demand for aircraft transport introduced jet engines to support large cargo and passengers. Consequently, this rise in innovation resulted in high volume engine noise due to the frequency of flights. After 1975, efforts to reduce aircraft noise eliminated the noise pollution for 90% of the population [4]. However, given the rapid increase in aircraft movements and consequently increase in noise exposure to larger populations, the advancement in noise reduction technologies has only been moderately increasing, leaving a requirement for in aeroacoustic modeling techniques and treatment strategies to compete with the demand for quiet subsonic flight [5]. Between the 1950s and 1960's aero gas turbine designs shifted to higher by pass ratios with two or three shafts. The high by pass ratio (HBP) fan utilized multiple stages of fans and air streams [1]. The efficiency of these engines rose with the availability of materials that are able to cool flows passing over the turbofan, thus slowing the overall jet velocity but maintaining the efficiency of the engine. One of the most popular configurations is the geared turbofan (GTF), the largest contributor to the noise on modern aircraft has been the fan upon take-off and landing. Although the use of the GTF has reduced the noise emissions by 75% [6], further noise reduction technologies to mitigate the noise associated to the turbofans geometric configuration and operation speeds. One of the most common techniques to reduce fan noise is to include the use of acoustic treatment along the walls of the turbomachine's nacelle.

Due to the increase in high-bypass-ratio of turbomachines, the newest models of engines have a significantly larger diameter and a shorter nacelle, leaving less room to place acoustic treatments in regions where it will be effective [7]. Figure 1-1 shows the evolution of directivity for turbomachines as the use of HBR fans became more popular. As these engines continue to develop, an increased understanding of sound propagation within the interstage of the engine is going to be needed due to flow be-

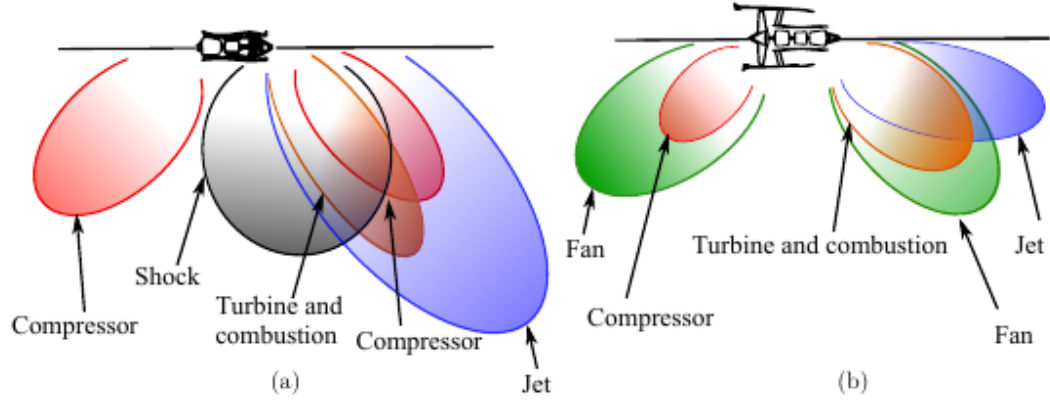


Figure 1-1: The evolution of the directivity and the relative levels of sources as a function of engine architecture (a) low bypass-ratio (b) high bypass ratio [1]

havior (high compressibility and rotational effects). While a turbomachine's general flow condition includes a series of axial, tangential, and radial velocity components that vary depending on the location of concern, the swirling flow between fan stages has been an area of interest due to the potential for acoustic treatment in a location previously avoided for its flow complexity. This work will explore how sound propagation is modeled and how the current state of code verification and validation currently stands. This introduction will describe how fluid mechanics is utilized to establish an aeroacoustic model for various ducted flows. It will also discuss how code verification is used in the computational and numerical fields but will show the need for the use of these code verification techniques for a frequency domain CAA code.

## 1.2 Statement of the of the research questions

### 1.2.1 What is already known?

In general, jet engine designers can model flow within a turbomachine with the Navier Stokes (N-S) Equations, a set of partial differential equations that describe

the mass, momentum and energy of a given viscous fluid, however these equations can be computationally expensive as they are used in the most general cases. For aeroacousticians, the N-S equations can be too complicated to identify sound generation and propagation because acoustic waves are low amplitude (only a fraction of atmospheric pressure) and are not strongly influenced by viscosity. As a result, it is common in practice to utilize the Linearized Euler equations (LEE), a closely related set of PDEs that model inviscid fluid, as they provide an approximation for higher Reynold number flows where viscosity does not play a critical role. A popular approach to modeling sound propagation within a flow is to “linearize” the Euler equations, which decomposes the flow solution into a mean and fluctuating component. The decomposition is done in a linear fashion because the sound propagation amplitude is small with respect to the mean flow, and their presence does not appreciably change the mean flow field. The LEE provides a system of linear equations where for uniform flow, the solution is a family of wavenumbers and radial mode shapes that arise from unsteady disturbances for flows within a cylindrical duct. Another method decomposes the flow into vortical and potential parts [8]. In either case, this presents an initial value problem which in limited cases can obtain analytical solutions for simplified mean flow. Once a mean flow contains a tangential component, the LEE equations must be solved numerically.

### **1.2.2 What is missing?/Why is it a problem?**

For uniform flows in a hard wall duct, the waves are categorized as vortical, entropical, and acoustic waves. The vortical and entropic waves solely convect with the mean flow, whereas the acoustic wave can propagate without damping or decay exponentially. However, for swirling flows, the waves are partially coupled and are not easily categorized due to an additional category of “nearly convecting” modes [9],[10]. Therefore, the families of waves must be found numerically [11] making the

ducted acoustic propagation in swirling flow a problem without an analytical solution but has a framework for a numerical solution.

### **1.2.3 The goal and significance of the investigation**

Swirling flow has been a difficult problem to investigate in comparison to flows parallel to the wall domain of a duct [12] because of the lack of an analytical solution and thus cannot be described from a single convective wave equation. However, the solution for sheared mean flows was first presented by Goldstein [13],[14]. Various special cases of swirling flow (free vortex and solid body swirl) was examined in [15] [9], [10]. In recent years verification and validation has been done given the rise in technologies capable of experimentally measuring the acoustic modes within a turbomachine [16]. This work aims offer additional insight to the verification and validation process by expanding on techniques used in this field.

## **1.3 Definition of the terms (if needed)**

## **1.4 Organization of research (Structure)**

This research aims to investigate the theoretical framework that is used to model ducted sound propagation within various flow fields and apply the “gold-standard” of code verification , the method of manufactured solutions (MMS) and method of exact solutions (MES) for the limited subset of equations where a solution is known, such as uniform mean flow.

The literature review in the next chapter will discuss the governing equations that are used to predict the acoustic behavior in a fluid flowing internally, followed by the research problem that arises in swirling flow, the objectives and questions, the significance and finally the limitations. The proposed research aims to determine

the impact of the numerical schemes used in the swirling flow problem and how it effects the family of waves that are produced from the problem formulation so a better understanding of the acoustic phenomena as the flow under goes a compressible rotational flow. The use of the method of manufactured solutions is used as a means of ensuring the code is correctly approximating the governing equations and will check the effect of the numerical schemes on the axial wavenumbers produced.

## 1.5 Research Questions and Hypothesis

- the problem that we're addressing
- being able to conduct component level code verification tests for the problem of characterizing the duct acoustics for flow using a LEE model.

why is it a problem? there is multiple ways of arriving at the same solution. This can be used to give a metric to either method for the various computational methods that may be needed to arrive at the final answer.

In the mid 90's,an aeroacoustics model for swirling flow had been proposed and has bypassed using a single PDE and has instead used an eigenvalue approach on the four governing flow equations. (Why Is this better? does this capture the problem differently? why not use the PDE alone instead...)

The proposed component verification from Kleb and Wood will be presented to address the characterization of modes and the presence of numerical ones. Using higher accuracy methods should further improve The result. another thing is to determine how many grid points are needed for each method

# Chapter 2

## Chapter 2: Literature Review

### 2.1 Introduction

#### 2.1.1 The problem to be addressed and its significance

The impact of swirling flow has been , there has been a concerted effort to model sound propagation under such conditions. This has lead to a number of publications that attempt to discern the acoustic signature of swirling flow through a cylindrical domain [9] , [10], [17], [18], [8] ,[19],[20], [21], [22], [23], [12], [24], [25], [26].

#### 2.1.2 Establish reasoning - i.e. point - of - view for reviewing the literature

A large amount of aircraft noise was reduced from 1975-2000, effectively eliminating the noise pollution for 90% of the population [4]. Since the early 2000's, the advancement in noise reduction technologies has been gradual, leaving a requirement for drastic improvement in aeroacoustic treatment strategies to compete with the demand of quiet subsonic flight. A previous theoretical review by Envia has been suggested that a non linear time domain computation could capture the source gener-

ation (incident turbulence) in addition to the broadband noise. Such a process would have the capabilities of solving all components of noise generation in an individual calculation [11]. This would at minimum, require an “LES-type” fidelity code, which can tend to be computationally expensive. A promising option is NASA GRC’s Broadband Aeroacoustic Stator Simulation (BASS). BASS is a high-order, high accuracy computational aeroacoustics (CAA) code which has been used to study non linear provides mean an extensive study of non linear phenomena in turbomachinery flow, and in particular, mechanisms of noise generation that are produced from unsteady disturbances. This code allows for a wide variety of finite differencing and time marching schemes as well as artificial dissipation methods. This effective computational tool allows for an in-depth modeling of realistic velocity profiles that would be representative of flow produced from a rotor blade row. In recent work, a new method of implementing realistic, three-dimensional rotor wakes free from acoustics was validated [27]. This provides a means of studying acoustic responses non linear swirling flows within pragmatic geometric configurations, while simultaneously allow for the modeling of sources generation produced from the incident turbulence.

Over the last 40 years, several studies have investigated the impact of swirling flow on the sound propagation with the use of the 3D linearized Euler equations, directly solving the unsteady equations as opposed to approximating the solutions to both steady and unsteady flow problems. Another NASA code, LINFLUX predict acoustic disturbances from blade movements in subsonic flows. While LINFLUX demonstrates capabilities to model three dimensional steady and unsteady flows, the computational time is larger compared to lower fidelity codes that only compute the unsteady portion of the problem. The benefit of such a code is beneficial to engine and liner designers who are interested in a wide range of configurations, requiring a parametric study. SWIRL [18], is a code that conducts an eigenmode analysis by assuming a constant radius annular or cylindrical duct with acoustically lined walls



using the linearized unsteady Euler equations. Such a code is needed to identify the modal content and can be used as a boundary condition with LINFLUX by using a mode matching technique. The goal of this theoretical review is to see the current state of low-fidelity frequency domain LEE codes and where the foundational model differs depending on the problem formulation.

### **2.1.3 Explain the order/sequence of the review**

This review will compare studies that have considered the applicability of unsteady linearized Euler equations on cylindrical and annular ducts. First the work of Kousen will be briefly summarized [18, 17]. Secondly, the alternate approach shown by Golubev and Atassi used in [19, 20] were also compared. These works have utilized a standard normal mode approach to determine the modal response of inviscid, compressible, swirling flow within a cylindrical and annular ducts. Results and findings have revealed three categories of associated wave - modes, acoustic, nearly convected, and nearly sonic. Detailed examination of the literature indicate that the hierarchical system was not initially apparent. A qualitative description of the numerical methods used to evaluate the eigensystem of solutions will be described. The use of the Method of Manufactured Solutions will also be described. While its use is widespread in the verification and validation community, very little aeroacoustic codes utilize the MMS to apply code verification. This review will discuss the procedures and guidelines associated with the MMS, and some specific measures that were taken to ensure that the guidelines were met and that the suggestions used in literature were expanded upon.

## 2.1.4 The theoretical foundation of conceptual framework

### 2.1.5 Work by Kousen

The study was expanded by [10, 28] who included cases of solid body swirl. Wundrow studied the swirling potential flows using Goldstein's disturbance velocity decomposition [13] using a numerical approach and found that the solutions were more accurate and found more efficiently [10]. Kousen expanded these efforts by including [17, 18] the effect unsteady disturbances in the presence of forced solid body-swirl and free-vortex flow without the use of potential flow theory. Using normal mode analysis along with a radial spatial differencing scheme, the wave modes produced within cylindrical and annular ducts was reported. Results show (figure 4.7) two distinct families of modes, purely convected and acoustic modes. The presence of axial shear in combination solid body flows can endue coupling between these modes, which in theory would not appear unless viscous terms were present in the eigenvalue analysis. Lack of available swirl flow results "hampered" validation attempts. However, this eigenvalue approach was utilized with a new quasi-3D formulation to find the axial wavenumbers from solid body flow was proposed in his next work .

In [18], A quasi 3D formulation was validated and used to predict the appearance of modes due to the interaction of a rotor with spatially uniform steady and unsteady flow. These modes were first classified by [29] as "spinning modes". In addition, further investigation was done on the results shown in [18]. The axial wavenumbers that were previously found to be purely convective were shown to be in part , "nearly convective" (shear) pressure modes. These were found to propagate in the axial direction with no loss in amplitude, thus never satisfying the cut-off condition.

## 2.2 Golubev and Atassi’s work

Similarly, a narrow annulus is once again studied but with a different theoretical and computational approach. The governing equations, similar to Wundrow [30] were still then linearized in terms of potential and rotation. As suggested by Case [31], a Fourier series analysis was used to conduct the normal mode analysis to find the corresponding wave numbers of the eigensystem. The findings show these fall into further classification which were previously denoted as purely convective and in part, nearly-convective wave modes. These two classifications of purely convective disturbance can be split into their “nearly-convected vorticity dominated” and “nearly-sonic pressure dominated” parts. These new results show the appearance of “nearly-sonic pressure dominated modes” which can propagate at varying phase speeds throughout the duct in both directions. The imposed Doppler shift from asymmetrical modes cause the sound propagate in the opposite direction of the mean flow swirl. A weak coupling relation relates the two and allows for the presence of vorticity - pressure mode coupling. Together, these nearly convected modes can be “identified with the purely convective gusts in a non swilirling flow”. For the second group, these “nearly convected” vorticity dominated modes are further split as these disturbances approach the *critical layer*, i.e. the location at which the viscous effects of the boundary layer begin to influence the coupling between modes. When both solid body and free vortex induced rotations are in the same direction, no instabilities arise from outside the critical layer. It was shown in later works that the influence of centrifugal and Coriolis forces created by the mean swirl prevent the decomposition of modes into their potential, rotational and entropic components. The paper ultimately proposes “ a generalized definition for incident rotational waves(gusts) is proposed which accounts for both the eigenmodes and the initial value solutions”

## 2.3 Review of the assessment of the numerical techniques

Kousen assessed the accuracy of the numerical discretization technique for a series of test cases using three sources [32] [33] and [34] ([10] [15] and [45] in Kousen's work [17] respectively). The results were assessed by using various literature comparisons. The methodology was presented of uniform mean axial flows, but results for hard wall cases were presented by computing the order of accuracy for the first four radial modes (See Figures 4.1-4.4), . (Explain why this is MES and offer MMS as a source of verification and explain that MES is validation [35] [36] ). For a uniform axial flow, the axial wavenumbers can be computed from an analytical solution, where one of the key input parameters are the zero crossings of the derivative of the Bessel Function of the first kind . The values are presented [37] and are often referred to as separation constants for a circumferential and radial mode pair ; which are needed to compute the solution of the convective wave equation.

The axial wavenumber is found by using second-order differential convective wave equation for pressure using a fourth order accurate Runge-Kutta(RK) method [18] which was done to check against the results in [38] (Table 4.1 and 4.2 in [18]). The output parameter was  $\gamma/k$ . Each axial wave number can then be used to compute the analytical radial mode using the exponential assumption. Axial wavenumbers from annular and cylindrical ducts with lined walls were compared to findings from Astley and Eversman [34] for uniform and sheared axial flow with liner (Table 4.3). The results taken were from a "high-order" RK scheme used. Axial wavenumbers from cylindrical ducts with hard walls were compared to findings from Shankar [32] in Table 4.4 of [18].

In recent years Maldonado et. al, [16] has made significant contributions in solution verification given the recent improvements in experimental measurement tech-

niques. The work has presented test cases for lined ducts that have been compared to Kousen [18], Nijboer [22] and Peake [25] and show excellent comparison. The goal of this work is to contribute these efforts by conducting the method of manufactured solutions to offer clarity in using techniques often used in other verification and validation (V&V) studies.

### **2.3.1 The research questions, hypotheses, foreshadowed problems, or conjectures**

While these results confirm the findings of SWIRL and other LEE codes, this does not check if the equations that were programmed were entered correctly. While an emphasis on solution verification is vital, it should be coupled with code verification to determine the robustness and consistency of the algorithm. The method of manufactured solutions combined with order of accuracy verification is often used as a gold standard of code verification [35] and has been shown to provide an estimate of discretization error that can be computed before the final answer is obtained. Since the mid 2000's, code verification literature has grown popular in the field of computational mathematics and physics due to its ability to conduct tests for numerical approximations of partial and ordinary differential equations. The MMS offers a means of “manufacturing” an arbitrary solution by define functions for each term in the governing equation. Common practices and guidelines are offered in [36] to choose the functions, but are phrased such that MMS can be widely applied. Since various numerical problems are unique in their treatment of spatial discretization, and boundary conditions, this work will describe the use of these guidelines and the nuances that have been taken to check the boundary condition and radial derivatives used in SWIRL.

Knupp in Code Verification by the MMS [36] provides guidelines for creating

## 2.4 Conclusion

- The conclusion summarizes the key findings of the review in general terms. Notable commonalities between works, whether favorable or not, may be included here.

This review discusses the development of the unsteady linearized equations, and how improvements in the modal analysis capture more families of mechanisms of noise generation within non-uniform swirling flow turbomachinery flow.

- This section is the reviewer's opportunity to justify a research proposal. Therefore, the idea should be clearly re-stated and supported according to the findings of the review.

While the literature presented offers a measure of verification and validation through the use of the Method of Exact Solutions, the Method of Manufactured Solutions offers a level of code verification which allows for error checking by computing the approximate order of accuracy for a given numerical scheme, which is independent of the final answer, which in this case is the axial wavenumber. The next chapter will outline the methodology and techniques used when applying MMS to SWIRL. The methods consist of unique treatment of boundary conditions using fairing functions as well as an example of using a summation to generate arbitrary functions as manufactured solutions which has the dual benefit of giving a large number of derivatives but allows for high gradients in specific locations along the domain of the MS. The use of open-source widely available functions in Python were used to symbolically create the MS and then used to generate FORTRAN code that will compute the MS for code comparison.

(Note: This literature review should be expanded to describe specific details in the methodologies and validation techniques reported by [18, 17, 20, 19].

# Chapter 3

## Chapter 3: Methods

### 3.1 Aerodynamic Models

#### 3.1.1 Steady Models



### 3.1.2 Setting up SWIRL's Aerodynamic Model

The Euler Equations in Cylindrical Form are,

$$\frac{\partial \rho}{\partial t} + v_r \frac{\partial \rho}{\partial r} + \frac{v_\theta}{r} \frac{\partial \rho}{\partial \theta} + v_x \frac{\partial \rho}{\partial x} + \rho \left( \frac{1}{r} \frac{\partial(rv_r)}{\partial r} + \frac{1}{r} \frac{\partial v_\theta}{\partial \theta} + \frac{\partial v_x}{\partial x} \right) = 0 \quad (3.1)$$

$$\frac{\partial v_r}{\partial t} + v_r \frac{\partial v_r}{\partial r} + \frac{v_\theta}{r} \frac{\partial v_r}{\partial \theta} - \frac{v_\theta^2}{r} + v_x \frac{\partial v_r}{\partial x} = -\frac{1}{\rho} \frac{\partial p}{\partial r} \quad (3.2)$$

$$\frac{\partial v_\theta}{\partial t} + v_r \frac{\partial v_\theta}{\partial r} + \frac{v_\theta}{r} \frac{\partial v_\theta}{\partial \theta} + \frac{v_r v_\theta}{r} + v_x \frac{\partial v_\theta}{\partial x} = -\frac{1}{\rho r} \frac{\partial p}{\partial \theta} \quad (3.3)$$

$$\frac{\partial v_x}{\partial t} + v_r \frac{\partial v_x}{\partial r} + \frac{v_\theta}{r} \frac{\partial v_x}{\partial \theta} + v_x \frac{\partial v_x}{\partial x} = -\frac{1}{\rho} \frac{\partial p}{\partial x} \quad (3.4)$$

$$\frac{\partial p}{\partial t} + v_r \frac{\partial p}{\partial r} + \frac{v_\theta}{r} \frac{\partial p}{\partial \theta} + v_x \frac{\partial p}{\partial x} + \gamma p \left( \frac{1}{r} \frac{\partial(rv_r)}{\partial r} + \frac{1}{r} \frac{\partial v_\theta}{\partial \theta} + \frac{\partial v_x}{\partial x} \right) = 0 \quad (3.5)$$

The following assumptions to simplify the aerodynamic model for the steady mean flow case,

- No flow in the radial direction. Consequentially, the flow is axisymmetric along the downstream direction.
- No surface or body forces
- Isentropic conditions

For steady flow, the continuity, momentum and entropy equations are

$$\nabla(\vec{V} \bar{\rho}) = 0 \quad (3.6)$$

$$(\vec{V} \cdot \nabla) \vec{V} = 0 \quad (3.7)$$

$$\nabla S = 0 \quad (3.8)$$

If the radial velocity is neglected, the velocity vector in cylindrical coordinates become,

$$\vec{V}(r, \theta, x) = V_x(r)\hat{e}_x + V_\theta(r)\hat{e}_\theta$$

## 3.2 Applying model to various flows

The LEE for flows with axial sheared flow, solid body and free vortex swirl were reviewed by [18], and most recently studied by [16].

### 3.2.1 Axial Shear Flow

In [18], axial sheared flows through a constant area duct was investigated. The only effect on the velocity gradient occurs along the x axis. All other primitive variables (pressure and density which is  $\propto$  speed of sound) are constant. As a result, the only changes that occur are in the x direction. This implies that  $\partial/\partial\theta = 0$ . For the conservation of mass,

$$\nabla(\vec{V}\bar{\rho}) = \left( \underbrace{\frac{\partial(\bar{\rho}v_r)}{\partial r}}_{v_r=0} + \underbrace{\frac{1}{r}\frac{\partial\bar{\rho}v_\theta}{\partial\theta}}_{\frac{\partial}{\partial\theta}} + \frac{\partial\bar{\rho}v_x}{\partial x} \right) = \frac{\partial\bar{\rho}v_x}{\partial x}$$

The conservation of momentum in the radial direction becomes:

$$(\vec{V} \cdot \nabla)\vec{V} = v_r \cancel{\frac{\partial v_r}{\partial r}} + \frac{v_\theta}{r} \cancel{\frac{\partial v_r}{\partial\theta}} - \frac{v_\theta^2}{r} + v_x \cancel{\frac{\partial v_r}{\partial x}} = -\frac{1}{\rho} \frac{\partial P}{\partial r}$$

$$\frac{v_\theta^2}{r} = \frac{1}{\rho} \frac{\partial P}{\partial r}$$

$$\frac{\rho v_\theta^2}{r} = \frac{\partial P}{\partial r}$$

For the  $\theta$  direction,

$$(\vec{V} \cdot \nabla)\vec{V} = v_r \cancel{\frac{\partial v_\theta}{\partial r}} + \frac{v_\theta}{r} \cancel{\frac{\partial v_\theta}{\partial\theta}} + \frac{v_r v_\theta}{r} + v_x \cancel{\frac{\partial v_\theta}{\partial x}} = -\frac{1}{\rho r} \frac{\partial P}{\partial\theta}$$

Dividing  $v_x$  to the other side,

$$\frac{\partial v_\theta}{\partial x} = 0$$

Similarly for the  $x$  direction,

$$\frac{\partial v_x}{\partial x} = 0$$

In regards to the entropy equation, having an isentropic flow,  $\nabla S = 0$  implies  $A^2 = \frac{\nabla \bar{P}}{\nabla \bar{\rho}}$

### 3.3 Accounting for solid body swirl

If the flow contains a swirling component, then the primitive variables are nonuniform through the flow, and mean flow assumptions are not valid. To account to this, we integrate the momentum equation in the radial direction with respect to the radius.

Equation (2.5) in [18] is

$$P = \int_{\tilde{r}}^1 \frac{\bar{\rho} V_\theta^2}{\tilde{r}} d\tilde{r}$$

where  $\tilde{r}$  is the radius dimensional radius normalized by the tip diameter  $r_t = r_{max}$

The dimensional form is,

$$\frac{\bar{\rho} v_\theta^2}{r} = \frac{\partial P}{\partial r}$$

By applying separation of variables, the expression for  $P$  can be found,

$$\int_r^{r_{max}} \frac{\bar{\rho} v_\theta^2}{r} dr = - \int_{P(r)}^{P(r_{max})} \partial P$$

Since  $\tilde{r} = r/r_{max}$  then,

$$r = \tilde{r} r_{max}$$

by taking total derivatives and applying chain rule,

$$dr = d(\tilde{r}r_{max}) = d(\tilde{r})r_{max}$$

Substituting these terms back in and evaluating the right hand side,

$$\int_{\tilde{r}}^1 \frac{\bar{\rho} v_{\theta}^2}{\tilde{r}} d\tilde{r} = P(1) - P(\tilde{r})$$

For reference the minimum value of  $\tilde{r}$  is

$$\sigma = \frac{r_{max}}{r_{min}}$$

The radial derivative of the speed of sound squared is then used to find the speed of sound in the cases where there is mean tangential component regardless of there being axial flow,

$$\frac{\partial A^2}{\partial r} = \frac{\partial}{\partial r} \left( \frac{\gamma P}{\rho} \right)$$

Using the quotient rule, the definition of the speed of sound is found to be ,

$$\begin{aligned} &= \frac{\partial P}{\partial r} \frac{\gamma \bar{\rho}}{\bar{\rho}^2} - \left( \frac{\gamma P}{\bar{\rho}^2} \right) \frac{\partial \bar{\rho}}{\partial r} \\ &= \frac{\partial P}{\partial r} \frac{\gamma}{\bar{\rho}} - \left( \frac{A^2}{\bar{\rho}} \right) \frac{\partial \bar{\rho}}{\partial r} \\ \text{Using } \partial P / A^2 = \partial \rho \rightarrow &= \frac{\partial P}{\partial r} \frac{\gamma}{\bar{\rho}} - \left( \frac{1}{\bar{\rho}} \right) \frac{\partial \bar{P}}{\partial r} \\ &\frac{\partial A^2}{\partial r} = \frac{\partial P}{\partial r} \frac{\gamma - 1}{\bar{\rho}} \\ \text{or..} &\frac{\bar{\rho}}{\gamma - 1} \frac{\partial A^2}{\partial r} = \frac{\partial P}{\partial r} \end{aligned}$$

Going back to the radial momentum equation , and rearranging the

$$\begin{aligned}\frac{\bar{\rho} v_\theta^2}{r} &= \frac{\partial P}{\partial r} \\ \frac{\bar{\rho} v_\theta^2}{r} &= \frac{\bar{\rho}}{\gamma - 1} \frac{\partial A^2}{\partial r} \\ \frac{v_\theta^2}{r} (\gamma - 1) &= \frac{\partial A^2}{\partial r} \\ \text{Dividing both sides by } A^2 \rightarrow \frac{M_\theta}{r} (\gamma - 1) &= \frac{\partial A^2}{\partial r} \frac{1}{A^2}\end{aligned}$$

$$\begin{aligned}\text{Integrating both sides } \int_r^{r_{max}} \frac{M_\theta}{r} (\gamma - 1) \partial r &= \int_{A^2(r)}^{A^2(r_{max})} \frac{1}{A^2} \partial A^2 \\ \int_r^{r_{max}} \frac{M_\theta^2}{r} (\gamma - 1) \partial r &= \ln(A^2(r_{max})) - \ln(A^2(r)) \\ \int_r^{r_{max}} \frac{M_\theta^2}{r} (\gamma - 1) \partial r &= \ln\left(\frac{A^2(r_{max})}{A^2(r)}\right)\end{aligned}$$

Defining non dimensional speed of sound  $\tilde{A} = \frac{A(r)}{A(r_{max})}$

$$\begin{aligned}\int_r^{r_{max}} \frac{M_\theta}{r} (\gamma - 1) \partial r &= \ln\left(\frac{1}{\tilde{A}^2}\right) \\ &= -2\ln(\tilde{A}) \\ \tilde{A}(r) &= \exp\left[-\int_r^{r_{max}} \frac{M_\theta}{r} \frac{(\gamma - 1)}{2} \partial r\right] \\ \text{replacing r with } \tilde{r} \rightarrow \tilde{A}(r) &= \exp\left[-\int_r^{r_{max}} \frac{M_\theta}{r} \frac{(\gamma - 1)}{2} \partial r\right] \\ \tilde{A}(\tilde{r}) &= \exp\left[\left(\frac{1 - \gamma}{2}\right) \int_{\tilde{r}}^1 \frac{M_\theta}{\tilde{r}} \partial \tilde{r}\right]\end{aligned}$$

### 3.3.1 Unsteady Models

## 3.4 No Flow

Starting with equation 2.28 (Wave Equation) in Kousen's paper,

$$\frac{1}{A^2} \frac{D^2 \tilde{p}}{Dt^2} - \nabla^2 \tilde{p} = 2\bar{\rho} \frac{dV_x}{dx} \frac{\partial \tilde{v}_r}{\partial x} \quad (3.9)$$

lets look at the no flow case. In the case of sheared flow,  $dV_x/dx = 0$  the right hand side will be zero

$$\frac{1}{A^2} \left( \frac{\partial^2 \tilde{p}}{\partial t^2} + \vec{V} \cdot \vec{\nabla}(\tilde{p}) \right) - \nabla^2 \tilde{p} = 0$$

Substituting the definitions for  $\nabla$  and  $\nabla^2$  in cylindrical coordinates gives,

$$\frac{1}{A^2} \left( \frac{\partial^2 \tilde{p}}{\partial t^2} + \vec{V} \cdot \left( \frac{\partial \tilde{p}}{\partial t} + \frac{1}{\tilde{r}} \frac{\partial \tilde{p}}{\partial \tilde{r}} + \frac{\partial \tilde{p}}{\partial \theta} + \frac{\partial \tilde{p}}{\partial x} \right) \right) - \left( \frac{\partial^2 \tilde{p}}{\partial t^2} + \frac{1}{\tilde{r}} \frac{\partial \tilde{p}}{\partial r} + \frac{1}{\tilde{r}^2} \frac{\partial^2 \tilde{p}}{\partial \theta^2} + \frac{\partial^2 \tilde{p}}{\partial x^2} \right) = 0$$

Setting  $\vec{V} = 0$ ,

$$\frac{1}{A^2} \left( \frac{\partial^2 \tilde{p}}{\partial t^2} \right) - \left( \frac{\partial^2 \tilde{p}}{\partial t^2} + \frac{1}{\tilde{r}} \frac{\partial \tilde{p}}{\partial r} + \frac{1}{\tilde{r}^2} \frac{\partial^2 \tilde{p}}{\partial \theta^2} + \frac{\partial^2 \tilde{p}}{\partial x^2} \right) = 0$$

Recall,  $\tilde{p} = p/\bar{\rho}A^2$ . To dimensionalize the equation, this is substituted and both sides are multiplied by  $\bar{\rho}A^2$ ,

$$\frac{1}{A^2} \left( \frac{\partial^2 p}{\partial t^2} \right) - \left( \frac{\partial^2 p}{\partial t^2} + \frac{1}{\tilde{r}} \frac{\partial p}{\partial r} + \frac{1}{\tilde{r}^2} \frac{\partial^2 p}{\partial \theta^2} + \frac{\partial^2 p}{\partial x^2} \right) = 0$$

The process of separation of variables (separation indeterminatarum) was first written and formalized by John Bernoulli in a letter to Leibniz. The method of separation of variables requires an assumed solution as well as initial and boundary conditions. For a partial differential equation, the assumed solution can be a linear combination of solutions to a system of ordinary differential equations that comprises the partial differential equation. Since  $p$  is a function of four variables, the solution is assumed to be a linear combination of four solutions. Each solution is assumed to be Euler's identity, a common ansatz for linear partial differential equations and boundary conditions.

Defining,

$$p(x, r, \theta, t) = X(x)R(r)\Theta(\theta)T(t) \tag{3.10}$$

where,

$$X(x) = A_1 e^{ik_x x} + B_1 e^{-ik_x x}$$

$$\Theta(\theta) = A_2 e^{ik_\theta \theta} + B_2 e^{-ik_\theta \theta}$$

$$T(t) = A_3 e^{i\omega t} + B_3 e^{-i\omega t}$$

The next step is to rewrite the wave equation in terms of  $X$ ,  $R$ ,  $\Theta$ , and  $T$ . To further simplify the result, each term is divided by  $p$ . Before the substitution, the derivatives of the assumed solutions need to be evaluated.



### 3.4.0.1 Temporal Derivatives

$$\begin{aligned}\frac{\partial p}{\partial t} &= \frac{\partial}{\partial t} (XR\Theta T) \\ &= XR\Theta \frac{\partial T}{\partial t}\end{aligned}$$

$$\begin{aligned}\frac{1}{p} \frac{\partial p}{\partial t} &= \frac{1}{XR\Theta T} \left( XR\Theta \frac{\partial T}{\partial t} \right) \\ &= \frac{1}{T} \frac{\partial T}{\partial t}\end{aligned}$$

$$\begin{aligned}\frac{\partial^2 p}{\partial t^2} &= \frac{\partial^2}{\partial t^2} (XR\Theta T) \\ &= XR\Theta \frac{\partial^2 T}{\partial t^2}\end{aligned}$$

$$\begin{aligned}\frac{1}{p} \frac{\partial^2 p}{\partial t^2} &= \frac{1}{XR\Theta T} \left( XR\Theta \frac{\partial^2 T}{\partial t^2} \right) \\ &= \frac{1}{T} \frac{\partial^2 T}{\partial t^2}\end{aligned}$$

$$\begin{aligned}\frac{\partial T}{\partial t} &= \frac{\partial}{\partial t} (A_3 e^{i\omega t} + B_3 e^{-i\omega t}) \\ &= \frac{\partial}{\partial t} (A_3 e^{i\omega t}) + \frac{\partial}{\partial t} (B_3 e^{-i\omega t}) \\ &= i\omega A_3 e^{i\omega t} - i\omega B_3 e^{i\omega t}\end{aligned}$$

$$\begin{aligned}
\frac{\partial^2 T}{\partial t^2} &= \frac{\partial^2}{\partial t^2} (i\omega A_3 e^{i\omega t} + i\omega B_3 e^{-i\omega t}) \\
&= \frac{\partial^2}{\partial t^2} (i\omega A_3 e^{i\omega t}) + \frac{\partial^2}{\partial t^2} (-i\omega B_3 e^{-i\omega t}) \\
&= (i\omega)^2 A_3 e^{i\omega t} - (i\omega)^2 B_3 e^{i\omega t}
\end{aligned}$$

$$\begin{aligned}
\frac{1}{T} \frac{\partial^2 T}{\partial t^2} &= (i\omega)^2 \\
&= -\omega^2
\end{aligned}$$

### 3.4.0.2 Radial Derivatives

$$\begin{aligned}
\frac{\partial p}{\partial r} &= \frac{\partial}{\partial r} (XR\Theta T) \\
&= X\Theta T \frac{\partial R}{\partial r}
\end{aligned}$$

$$\begin{aligned}
\frac{1}{p} \frac{\partial p}{\partial r} &= \frac{1}{XR\Theta T} \left( X\Theta T \frac{\partial R}{\partial r} \right) \\
&= \frac{1}{R} \frac{\partial R}{\partial r}
\end{aligned}$$

$$\begin{aligned}
\frac{\partial^2 p}{\partial r^2} &= \frac{\partial^2}{\partial r^2} (XR\Theta T) \\
&= X\Theta T \frac{\partial^2 R}{\partial r^2}
\end{aligned}$$

$$\begin{aligned}\frac{1}{p} \frac{\partial^2 p}{\partial r^2} &= \frac{1}{XR\Theta T} \left( X\Theta T \frac{\partial^2 R}{\partial r^2} \right) \\ &= \frac{1}{R} \frac{\partial^2 R}{\partial r^2}\end{aligned}$$

The radial derivatives will be revisited once the remaining derivatives are evaluated,

### 3.4.0.3 Tangential Derivatives

$$\begin{aligned}\frac{\partial p}{\partial \theta} &= \frac{\partial}{\partial t} (XR\Theta T) \\ &= XR T \frac{\partial \Theta}{\partial \theta}\end{aligned}$$

$$\begin{aligned}\frac{1}{p} \frac{\partial p}{\partial \theta} &= \frac{1}{XR\Theta T} \left( XR\Theta \frac{\partial T}{\partial \theta} \right) \\ &= \frac{1}{\Theta} \frac{\partial \Theta}{\partial \theta}\end{aligned}$$

$$\begin{aligned}\frac{\partial^2 p}{\partial \theta^2} &= \frac{\partial^2}{\partial \theta^2} (XR\Theta T) \\ &= XR T \frac{\partial^2 \Theta}{\partial \theta^2}\end{aligned}$$

$$\begin{aligned}\frac{1}{p} \frac{\partial^2 p}{\partial \theta^2} &= \frac{1}{XR\Theta T} \left( XR T \frac{\partial^2 \Theta}{\partial \theta^2} \right) \\ &= \frac{1}{\Theta} \frac{\partial^2 \Theta}{\partial \theta^2}\end{aligned}$$

$$\begin{aligned}
\frac{\partial \Theta}{\partial \theta} &= \frac{\partial}{\partial \theta} (A_2 e^{ik_\theta \theta} + B_2 e^{-ik_\theta \theta}) \\
&= \frac{\partial}{\partial \theta} (A_2 e^{ik_\theta \theta}) + \frac{\partial}{\partial \theta} (B_2 e^{-ik_\theta \theta}) \\
&= ik_\theta A_2 e^{ik_\theta \theta} - ik_\theta B_2 e^{-ik_\theta \theta}
\end{aligned}$$

$$\begin{aligned}
\frac{\partial^2 \Theta}{\partial \theta^2} &= \frac{\partial^2}{\partial \theta^2} (ik_\theta A_2 e^{ik_\theta \theta} - ik_\theta B_2 e^{-ik_\theta \theta}) \\
&= \frac{\partial^2}{\partial \theta^2} (ik_\theta A_2 e^{ik_\theta \theta}) + \frac{\partial^2}{\partial \theta^2} (-ik_\theta B_2 e^{-ik_\theta \theta}) \\
&= (ik_\theta)^2 A_2 e^{ik_\theta \theta} - (ik_\theta)^2 B_2 e^{-ik_\theta \theta}
\end{aligned}$$

$$\begin{aligned}
\frac{1}{\Theta} \frac{\partial^2 \Theta}{\partial \theta^2} &= (ik_\theta)^2 \\
&= -k_\theta^2
\end{aligned}$$

#### 3.4.0.4 Axial Derivatives

$$\begin{aligned}
\frac{\partial p}{\partial x} &= \frac{\partial}{\partial x} (XR\Theta T) \\
&= R\Theta T \frac{\partial X}{\partial x}
\end{aligned}$$

$$\begin{aligned}\frac{1}{p} \frac{\partial p}{\partial x} &= \frac{1}{XR\Theta T} \left( R\Theta \frac{\partial X}{\partial x} \right) \\ &= \frac{1}{X} \frac{\partial X}{\partial x}\end{aligned}$$

$$\begin{aligned}\frac{\partial^2 p}{\partial x^2} &= \frac{\partial^2}{\partial x^2} (XR\Theta T) \\ &= R\Theta T \frac{\partial^2 X}{\partial x^2}\end{aligned}$$

$$\begin{aligned}\frac{1}{p} \frac{\partial^2 p}{\partial x^2} &= \frac{1}{XR\Theta T} \left( R\Theta T \frac{\partial^2 X}{\partial x^2} \right) \\ &= \frac{1}{X} \frac{\partial^2 X}{\partial x^2}\end{aligned}$$

$$\begin{aligned}\frac{\partial X}{\partial x} &= \frac{\partial}{\partial t} (A_3 e^{ik_x t} + B_3 e^{-i\omega t}) \\ &= \frac{\partial}{\partial t} (A_1 e^{ik_x x}) + \frac{\partial}{\partial t} (B_1 e^{-ik_x x}) \\ &= ik_x A_1 e^{ik_x x} - ik_x B_1 e^{ik_x x}\end{aligned}$$

$$\begin{aligned}\frac{\partial^2 X}{\partial x^2} &= \frac{\partial^2}{\partial x^2} (ik_x A_1 e^{ik_x x} + ik_x B_1 e^{-ik_x x}) \\ &= \frac{\partial^2}{\partial x^2} (ik_x A_1 e^{ik_x x}) + \frac{\partial^2}{\partial x^2} (-ik_x B_1 e^{-ik_x x}) \\ &= (ik_x)^2 A_1 e^{ik_x x} - (ik_x)^2 B_1 e^{ik_x x}\end{aligned}$$

$$\begin{aligned}\frac{1}{X} \frac{\partial^2 X}{\partial x^2} &= (ik_x)^2 \\ &= -k_x^2\end{aligned}$$

Substituting this back into the wave equation yields ,

$$\frac{1}{A^2} \left( \frac{\partial^2 p}{\partial t^2} \right) = \left( \frac{\partial^2 p}{\partial t^2} + \frac{1}{\tilde{r}} \frac{\partial p}{\partial r} + \frac{1}{\tilde{r}^2} \frac{\partial^2 p}{\partial \theta^2} + \frac{\partial^2 p}{\partial x^2} \right)$$

$$\frac{1}{A^2} \frac{1}{T} \frac{\partial^2 T}{\partial t^2} = \frac{1}{R} \frac{\partial^2 R}{\partial r^2} + \frac{1}{r} \frac{1}{R} \frac{\partial R}{\partial r} + \frac{1}{r^2} \frac{1}{\Theta} \frac{\partial \Theta}{\partial \theta} + \frac{1}{X} \frac{\partial^2 X}{\partial x^2} \quad (3.11)$$

Notice that each term is only a function of its associated independent variable. So, if we vary the time, only the term on the left-hand side can vary. However, since none of the terms on the right-hand side depend on time, that means the right-hand side cannot vary, which means that the ratio of time with its second derivative is independent of time. The practical upshot is that each of these terms is constant, which has been shown. The wave numbers are the *separation constants* that allow the PDE to be split into four separate ODE's. Substituting the separation constants into Equation (3.11) gives,

$$-\frac{\omega^2}{A^2} = \frac{1}{R} \left( \frac{\partial^2 R}{\partial r^2} + \frac{1}{r} \frac{\partial R}{\partial r} \right) - \frac{k_\theta^2}{r^2} - k_x^2 \quad (3.12)$$

Note that the dispersion relation states  $\omega = kA$

$$\frac{1}{R} \left( \frac{\partial^2 R}{\partial r^2} + \frac{1}{r} \frac{\partial R}{\partial r} \right) - \frac{k_\theta^2}{r^2} - k_x^2 + k^2 = 0 \quad (3.13)$$

The remaining terms are manipulated to follow the same form as *Bessel's Differential*

Equation ,

$$x^2 \frac{d^2 y}{dx^2} + x \frac{dy}{dx} + (x^2 - n^2)y = 0 \quad (3.14)$$

The general solution to Bessel's differential equation is a linear combination of the Bessel functions of the first kind,  $J_n(x)$  and of the second kind,  $Y_n(x)$  [?]. The subscript  $n$  refers to the order of Bessel's equation.

$$y(x) = AJ_n(x) + BY_n(x) \quad (3.15)$$

By rearranging Equation (3.13), a comparison can be made to Equation (3.14) to show that the two equations are of the same form.

The first step is to revisit the radial derivatives that have not been addressed. As was done for the other derivative terms, the radial derivatives will also be set equal to a separation constant,  $-k_r^2$ .

$$\underbrace{\frac{1}{R} \left( \frac{\partial^2 R}{\partial r^2} + \frac{1}{r} \frac{\partial R}{\partial r} \right) - \frac{k_\theta^2}{r^2}}_{-k_r^2} - k_x^2 + k^2 = 0 \quad (3.16)$$

The reader may be curious as to why the tangential separation constant  $k_\theta$  is included within the definition of the radial separation constant.

Recall the ODE for the tangential direction,

$$\begin{aligned} \frac{\partial \Theta}{\partial \theta} \frac{1}{\Theta} &= -k_\theta^2 \\ \frac{\partial \Theta}{\partial \theta} \frac{1}{\Theta} + \Theta k_\theta^2 &= 0 \end{aligned}$$

where the solution is more or less,

$$\Theta(\theta) = e^{ik_\theta\theta}$$

In order to have non trivial, sensible solutions, the value of  $\Theta(0)$  and  $\Theta(2\pi)$  need to be the same, and this needs to be true for any multiple of  $2\pi$  for a fixed  $r$ . Taking  $\Theta$  to be one, a unit circle, it can be shown that the domain is only going to be an integer multiple. Therefore, there is an implied periodic azimuthal boundary condition, i.e.  $0 < \theta \leq 2\pi$  and  $k_\theta = m$ .

Continuing with the radial derivatives...

$$-k_r^2 = \frac{1}{R} \left( \frac{\partial^2 R}{\partial r^2} + \frac{1}{r} \frac{\partial R}{\partial r} \right) - \frac{m^2}{r^2}$$

To further simplify, the chain rule is used to do a change of variables,  $x = k_r r$

$$\begin{aligned} \frac{\partial R}{\partial r} &= \frac{dR}{dx} \frac{dx}{dr} \\ &= \frac{dR}{dx} \frac{d}{dr} (k_r r) \\ &= \frac{dR}{dx} k_r \end{aligned}$$

$$\begin{aligned} \frac{\partial^2 R}{\partial r^2} &= \frac{d^2 R}{dx^2} \left( \frac{dx}{dr} \right)^2 + \frac{dR}{dx} \frac{d^2 x}{dr^2} \\ &= \frac{d^2 R}{dx^2} \frac{d}{dr} k_r^2 + k_r \frac{d^2 r}{dr^2} \\ &= \frac{d^2 R}{dx^2} \frac{d}{dr} k_r^2 \end{aligned}$$



Substituting this into Equation (3.13),

$$\left( \frac{d^2 R}{dx^2} k_r^2 + \frac{1}{r} \frac{d^2 R}{dx^2} k_r \right) + \left( k_r^2 - \frac{m^2}{r^2} \right) R \quad (3.17)$$

Dividing Equation 3.17 by  $k_r^2$ ,

$$\left( \frac{d^2 R}{dx^2} + \frac{1}{k_r r} \frac{d^2 R}{dx^2} \right) + \left( 1 - \frac{m^2}{k_r^2 r^2} \right) R \quad (3.18)$$

$$\left( \frac{d^2 R}{dx^2} + \frac{1}{x^2} \frac{d^2 R}{dx^2} \right) + \left( 1 - \frac{m^2}{x^2} \right) R \quad (3.19)$$

Multiplying Equation (3.19) by  $x^2$  gives,

$$\frac{d^2 R}{dr^2} x^2 + \frac{dR}{dr} x + (x^2 - m^2) R \quad (3.20)$$

which matches the form of Bessel's equation

Therefore, the solution goes from this,

$$y(x) = AJ_n(x) + BY_n(x) \quad (3.21)$$

to this,

$$R(r) = (AJ_n(k_r r) + BY_n(k_r r)) \quad (3.22)$$

where the coefficients  $A$  and  $B$  are found after applying radial boundary conditions.

### 3.4.0.5 Hard Wall boundary condition

$$\begin{aligned}\frac{\partial p}{\partial r}|_{r=r_{min}} = \frac{\partial p}{\partial r}|_{r=r_{max}} = 0 &\rightarrow \frac{\partial}{\partial r}(X\Theta TR) = 0 \\ X\Theta T \frac{\partial R}{\partial r} &= 0 \\ \frac{\partial R}{\partial r} &= 0\end{aligned}$$

where,

$$\frac{\partial R}{\partial r}|_{r_{min}} = AJ'_n(k_r r_{min}) + BY'_n(k_r r_{min}) = 0 \rightarrow B = -A \frac{J'_n(k_r r_{min})}{Y'_n(k_r r_{min})}$$

$$\begin{aligned}\frac{\partial R}{\partial r} &= AJ'_n(k_r r_{max}) + BY'_n(k_r r_{max}) = 0 \\ &= AJ'_n(k_r r_{max}) - A \frac{J'_n(k_r r_{min})}{Y'_n(k_r r_{min})} Y'_n(k_r r_{max}) = 0 \\ &= \frac{J'_n(k_r r_{min})}{J'_n(k_r r_{max})} - \frac{Y'_n(k_r r_{min})}{Y'_n(k_r r_{max})} = 0\end{aligned}$$

where  $k_r r$  are the zero crossings for the derivatives of the Bessel functions of the first and second kind.

In summary, the wave equation for no flow in a hollow duct with hard walls is obtained from Equation (3.16).

$$k^2 = k_r^2 + k_x^2 \quad (3.23)$$

Solving for the axial wavenumber gives,

### 3.5 Uniform Flow

To get the same equation but for uniform flow, the same procedure can be followed.

Starting with Equation 2.27 redimensionalized,

$$\frac{d^2 \tilde{p}}{d\tilde{r}^2} + \frac{1}{\tilde{r}} \frac{d\tilde{p}}{d\tilde{r}} + \frac{2\bar{\gamma} \left( \frac{dm_x}{d\tilde{r}} \right)}{(k - \bar{\gamma}m_x)} \frac{d\tilde{p}}{d\tilde{r}} + \left[ (k - \bar{\gamma}m_x)^2 - \frac{m^2}{\tilde{r}^2} - \bar{\gamma}^2 \right] \tilde{p}$$

Let's separate the new terms from the old ones,

$$\frac{d^2 \tilde{p}}{d\tilde{r}^2} + \frac{1}{\tilde{r}} \frac{d\tilde{p}}{d\tilde{r}} + \frac{2\bar{\gamma} \left( \frac{dm_x}{d\tilde{r}} \right)}{(k - \bar{\gamma}m_x)} \frac{d\tilde{p}}{d\tilde{r}} + \left[ (k - \bar{\gamma}m_x)^2 - \frac{m^2}{\tilde{r}^2} - \bar{\gamma} \right] \tilde{p}$$

Recalling the non-dimensional definitions,

$$\begin{aligned} \tilde{p} &= \frac{p}{\bar{\rho}A^2} \\ \tilde{r} &= \frac{r}{r_T} \\ \frac{\partial \tilde{p}}{\partial \tilde{r}} &= \frac{\partial \tilde{p}}{\partial r} \frac{\partial r}{\partial \tilde{r}} \\ &= \frac{\partial \tilde{p}}{\partial r} \frac{\partial}{\partial \tilde{r}} (\tilde{r}r_T) \\ &= \frac{\partial \tilde{p}}{\partial r} r_T \\ \frac{\partial^2 \tilde{p}}{\partial \tilde{r}^2} &= \frac{\partial^2 \tilde{p}}{\partial r^2} (r_T)^2 + \frac{\partial \tilde{p}}{\partial r} \frac{\partial^2 r}{\partial \tilde{r}^2} \\ &= \frac{\partial^2 \tilde{p}}{\partial r^2} (r_T)^2 \end{aligned}$$

$$\begin{aligned}\frac{\partial}{\partial r} \left( \frac{p}{\bar{\rho} A^2} \right) &= \frac{\left( \frac{\partial}{\partial r} (p) \bar{\rho} A^2 - \underbrace{\frac{\partial \bar{\rho} A^2}{\partial r} p}_0 \right)}{(\bar{\rho} A^2)^2} \\ &= \frac{1}{\bar{\rho} A^2} \frac{\partial p}{\partial r}\end{aligned}$$

$$\frac{d^2 \tilde{p}}{d\tilde{r}^2} + \frac{1}{\tilde{r}} \frac{d\tilde{p}}{d\tilde{r}} - \frac{m^2}{\tilde{r}^2} \tilde{p} - \bar{\gamma}^2 \tilde{p} + \frac{2\bar{\gamma} \left( \frac{dM_x}{d\tilde{r}} \right)}{(k - \bar{\gamma} M_x)} \frac{d\tilde{p}}{d\tilde{r}} + (k - \bar{\gamma} M_x)^2 \tilde{p}$$

If there is only uniform flow, then  $dM_x/dr = 0$ ,

$$\frac{d^2 \tilde{p}}{d\tilde{r}^2} + \frac{1}{\tilde{r}} \frac{d\tilde{p}}{d\tilde{r}} - \frac{m^2}{\tilde{r}^2} \tilde{p} - \bar{\gamma}^2 \tilde{p} + (k - \bar{\gamma} M_x)^2 \tilde{p}$$

Re-dimensionalizing,

$$\frac{1}{\bar{\rho} A^2} \left[ \frac{d^2 p}{dr} r_T^2 + \frac{r_T}{r} \frac{dp}{dr} r_T - \frac{m^2}{r^2} r_T^2 p - k_x^2 r_T^2 p \right] + \left( \frac{\omega}{A} r_T - k_x r_T M_x \right)^2 p$$

Expanding the last term and substituting  $\omega/A = k$

$$\frac{1}{\bar{\rho} A^2} \left[ \frac{d^2 p}{dr} r_T^2 + \frac{r_T}{r} \frac{dp}{dr} r_T - \frac{m^2}{r^2} r_T^2 p - k_x^2 r_T^2 p \right] + \left( r_T^2 (k^2 - 2k k_x M_x + k_x^2 M_x^2) \right) p$$

Canceling out  $r_T/\bar{\rho}A$  in every term

$$\frac{d^2 p}{dr} + \frac{1}{r} \frac{dp}{dr} + \left[ k^2 - 2k k_x M_x + k_x^2 M_x^2 - \frac{m^2}{r^2} - k_x^2 \right] p$$

Continue here,

Defining

$$-N^2 = k_x^2 M_x^2 - 2k k_x M_x - k_x^2$$

$$-N^2 = -(1 - M_x^2) k_x^2 - 2k k_x M_x$$

$$-N^2 = -\beta^2 k_x^2 - 2k k_x M_x$$

$$\frac{d^2 p}{dr} + \frac{1}{r} \frac{dp}{dr} + \left[ k^2 - N^2 - \frac{m^2}{r^2} \right] p$$

Let  $k_r^2 = k^2 - N^2$

$$\frac{d^2 p}{dr} + \frac{1}{r} \frac{dp}{dr} + \left[ k_r^2 - \frac{m^2}{r^2} \right] p$$

Looking at the radial wavenumber,

$$\begin{aligned} k_r^2 &= k^2 - N^2 \\ &= k^2 - \beta^2 k_x^2 - 2k k_x M_x \\ 0 &= -\beta^2 k_x^2 - (2M_x k) k_x + (k^2 - k_r^2) \end{aligned}$$

Where the roots to this equation are the axial wavenumber,

Applying the quadratic formula and taking

$$A = -\beta^2$$

$$B = -2M_x k$$

$$C = k^2 - k_r^2$$

Note B is negative when  $M_x$  is positive,

(I feel like N should change based on  $M'_x$ 's sign)

$$\begin{aligned} k_x &= \frac{2M_x k \pm \sqrt{4M_x^2 k^2 + 4\beta^2 (k^2 - k_r^2)}}{-2\beta^2} \\ &= \frac{-M_x k \pm \sqrt{k^2 - k_r^2}}{\beta^2} \end{aligned}$$

### 3.6 Annular Duct Axial Wavenumber solution

This needs to be proven,

In [?], the axial wavenumber for annular ducts is reported,

$$\frac{-(\omega - mM_\theta)M_x \pm \sqrt{(\omega - mM_\theta^2) - \beta (m^2 + \Gamma_{m,n}^2)}}{\beta^2}$$

where

$$\Gamma_{m,n} = \frac{n^2 \pi^2}{(r_{max} - r_{min})^2}$$

# Chapter 4

## Chapter 4: Numerical Models

### 4.1 Numerical Integration

### 4.2 Introduction

The Method of Manufactured Solutions (MMS) is a process for generating an analytical solution for a code that provides the numerical solution for a given domain. The goal of MMS is to establish a manufactured solution that can be used to establish the accuracy of the code within question. For this study, SWIRL, a code used to calculate the radial modes within an infinitely long duct is being validated through code verification. SWIRL accepts a given mean flow and uses numerical integration to obtain the speed of sound. The integration technique is found to be the composite trapezoidal rule through asymptotic error analysis.

For SWIRL, the absolute bare minimum requirement is to define the corresponding flow components for the domain of interest. SWIRL assumes no flow in the radial direction, leaving only two other components, axial and tangential for a 3D cylindrical domain. Since SWIRL is also non dimensionalized, the mean flow components are defined using the Mach number. SWIRL uses the tangential mach number to obtain the speed of sound using numerical integration. The speed of sound is then used to

find the rest of the primitive variables for the given flow.



### 4.3 Methods

SWIRL is a linearized Euler equations of motion code that calculates the axial wavenumber and radial mode shapes from small unsteady disturbances in a mean flow. The mean flow varies along the axial and tangential directions as a function of radius. The flow domain can either be a circular or annular duct, with or without acoustic liner. SWIRL was originally written by Kousen [insert ref].

The SWIRL code requires two mean flow parameters as a function of radius,  $M_x$ , and  $M_\theta$ . Afterwards, the speed of sound,  $\tilde{A}$  is calculated by integrating  $M_\theta$  with respect to  $r$ . To verify that SWIRL is handling and returning the accompanying mean flow parameters, the error between the mean flow input and output variables are computed. Since the trapezoidal rule is used to numerically integrate  $M_\theta$ , the discretization error and order of accuracy is computed. Since finite differencing schemes are to be used on the result of this integration, it is crucial to accompany the integration with methods of equal or less order of accuracy. This will be determined by applying another MMS on the eigenproblem which will also have an order of accuracy.

### 4.3.1 Theory

To relate the speed of sound to a given flow, the radial momentum equation is used. If the flow contains a swirling component, then the primitive variables are nonuniform through the flow, and mean flow assumptions are not valid.

$$\frac{\partial v_r}{\partial t} + v_r \frac{\partial v_r}{\partial r} + \frac{v_\theta}{r} \frac{\partial v_\theta}{\partial \theta} - \frac{v_\theta^2}{r} v_x \frac{\partial v_r}{\partial x} = \frac{1}{\rho} \frac{\partial P}{\partial r}$$

To account to for this, the radial momentum is simplified by assuming the flow is steady, the flow has no radial component. In addition, the viscous and body forces are neglected. Then the radial pressure derivative term is set equal to the dynamic pressure term. Separation of variables is applied.

$$\frac{v_\theta^2}{r} = \frac{1}{\rho} \frac{\partial P}{\partial r}$$

$$P = \int_r^{r_{max}} \frac{\rho V_\theta^2}{r}$$

To show the work, we will start with the dimensional form of the equation and differentiate both sides. Applying separation of variables,

$$\int_r^{r_{max}} \frac{\bar{\rho} v_\theta^2}{r} \partial r = - \int_{P(r)}^{P(r_{max})} \partial p.$$

Since  $\tilde{r} = r/r_{max}$ ,

$$r = \tilde{r} r_{max}.$$

Taking total derivatives (i.e. applying chain rule),

$$dr = d(\tilde{r} r_{max}) = d(\tilde{r}) r_{max},$$

Substituting these back in and evaluating the right hand side,

$$\int_{\tilde{r}}^1 \frac{\bar{\rho} v_{\theta}^2}{\tilde{r}} \partial \tilde{r} = P(1) - P(\tilde{r})$$

For reference the minimum value of  $\tilde{r}$  is,

$$\sigma = \frac{r_{max}}{r_{min}}$$

For the radial derivative, the definition of the speed of sound is utilized,

$$\frac{\partial A^2}{\partial r} = \frac{\partial}{\partial r} \left( \frac{\gamma P}{\rho} \right).$$

Using the quotient rule, the definition of the speed of sound is extracted,

$$\begin{aligned} &= \frac{\partial P}{\partial r} \frac{\gamma \bar{\rho}}{\bar{\rho}^2} - \left( \frac{\gamma P}{\bar{\rho}^2} \right) \frac{\partial \bar{\rho}}{\partial r} \\ &= \frac{\partial P}{\partial r} \frac{\gamma}{\bar{\rho}} - \left( \frac{A^2}{\bar{\rho}} \right) \frac{\partial \bar{\rho}}{\partial r} \end{aligned}$$

Using isentropic condition  $\partial P/A^2 = \partial \rho$ ,

$$\begin{aligned} &= \frac{\partial P}{\partial r} \frac{\gamma}{\bar{\rho}} - \left( \frac{1}{\bar{\rho}} \right) \frac{\partial P}{\partial r} \\ \frac{\partial A^2}{\partial r} &= \frac{\partial P}{\partial r} \frac{\gamma - 1}{\bar{\rho}} \end{aligned}$$

$$\frac{\bar{\rho}}{\gamma - 1} \frac{\partial A^2}{\partial r} = \frac{\partial P}{\partial r}$$

Going back to the radial momentum equation, and rearranging the terms will simplify the expression. The following terms are defined to start the nondimensionalization.

$$\begin{aligned}
M_\theta &= \frac{V_\theta}{A} \\
\tilde{r} &= \frac{r}{r_{max}} \\
\tilde{A} &= \frac{A}{A_{r,max}} \\
A &= \tilde{A}A_{r,max} \\
r &= \tilde{r}r_{max} \\
\frac{\partial}{\partial r} &= \frac{\partial \tilde{r}}{\partial r} \frac{\partial}{\partial \tilde{r}} \\
&= \frac{1}{r_{max}} \frac{\partial}{\partial \tilde{r}}
\end{aligned}$$

Dividing by  $A$ ,

$$\frac{M_\theta^2}{r} (\gamma - 1) = \frac{\partial A^2}{\partial r} \frac{1}{A^2}$$

Now there is two options, either find the derivative of  $\tilde{A}$  or the integral of  $M_\theta$  with respect to  $r$ .

1. Defining non dimensional speed of sound  $\tilde{A} = \frac{A(r)}{A(r_{max})}$

$$\begin{aligned}
\int_r^{r_{max}} \frac{M_\theta}{r} (\gamma - 1) \partial r &= \ln \left( \frac{1}{\tilde{A}^2} \right) \\
&= -2 \ln(\tilde{A}) \\
\tilde{A}(r) &= \exp \left[ - \int_r^{r_{max}} \frac{M_\theta (\gamma - 1)}{r} \partial r \right] \\
\text{replacing } r \text{ with } \tilde{r} \rightarrow \tilde{A}(r) &= \exp \left[ - \int_r^{r_{max}} \frac{M_\theta (\gamma - 1)}{r} \partial r \right] \\
\tilde{A}(\tilde{r}) &= \exp \left[ \left( \frac{1 - \gamma}{2} \right) \int_{\tilde{r}}^1 \frac{M_\theta}{\tilde{r}} \partial \tilde{r} \right]
\end{aligned}$$

2. Or we can differentiate

Solving for  $M_\theta$ ,

$$M_\theta^2 = \frac{\partial A^2}{\partial r} \frac{r}{A^2 (\gamma - 1)}$$

Nondimensionalizing and substituting,

$$\begin{aligned}
M_\theta^2 \frac{(\gamma - 1)}{\tilde{r} r_{max}} &= \frac{1}{(\tilde{A} A_{r,max})^2} \frac{A_{r,max}^2}{r_{max}} \frac{\partial \tilde{A}^2}{\partial \tilde{r}} \\
M_\theta^2 \frac{(\gamma - 1)}{\tilde{r}} &= \frac{1}{\tilde{A}^2} \frac{\partial \tilde{A}^2}{\partial \tilde{r}} \\
M_\theta &= \sqrt{\frac{\tilde{r}}{(\gamma - 1) \tilde{A}^2} \frac{\partial \tilde{A}^2}{\partial \tilde{r}}} \tag{4.1}
\end{aligned}$$

### 4.3.2 Procedure

There are a few constraints and conditions that must be followed in order for the analytical function to work with SWIRL,

- The mean flow and speed of sound must be real and positive. This will occur if a speed of sound is chosen such that the tangential mach number is imaginary
- The derivative of the speed of sound must be positive
- Any bounding constants used with the mean flow should not allow the total Mach number to exceed one.
- the speed of sound should be one at the outer radius of the cylinder

Given these constraints,  $\tanh(r)$  is chosen as a function since it can be modified to meet the conditions above. Literature (The tanh method: A tool for solving certain classes of nonlinear evolution and wave equations) is a paper that demonstrates the strength of using tanh functions. One additional benefit of  $\tanh(r)$  is that it is bounded between one and negative one, i.e.

- As  $r \rightarrow \infty$   $\tanh(r) \rightarrow 1$
- As  $-r \rightarrow -\infty$   $\tanh(r) \rightarrow -1$

To test the numerical integration method,  $M_\theta$  is defined as a result of differentiating the speed of sound,  $A$ . This is done opposed to integrating  $M_\theta$  analytically. However, an analytical function can be defined for  $M_\theta$ , which can then be integrated to find what  $\tilde{A}$  should be. Instead, the procedure of choice is to back calculate what the appropriate  $M_\theta$  is for a given expression for  $\tilde{A}$ . Since it is easier to take derivatives, we will solve for  $M_\theta$  using Equation 4.1 ,

### 4.3.3 Tanh Summaion Formulation

The goal is generate an MS with a number of “stairs” that is bounded between zero and one. Here’s what my focus group ideas are,

$$1 = R + L$$

where, 1 is a constraint, and R and L are the two waves when summed need to cancel if it were the exact same amplitude & opposite sign

so ,

$$R + L = \tanh(x) + -\tanh(x) = 0$$

or in our case,

$$R + L = \tanh(x) + -\tanh(x) = 1$$

We can tweak this by adding knobs by adding “knobs” A and B. If we dont want the total to not exceed one then,  $A_j + A_{j+1} \cdots A_{last} = 1$ .  $B_1$  changes the steepnes of the kink that we want. In order to generalize this,

$$\bar{A} = \sum_{j=1}^n R_{ij} + \sum_{j=1}^n L_{ij}$$

where,

$$R_{ij} = A_j \tanh(B_j(x_i - x_j))$$

$$L_{ij} = A_j \tanh(B_j(x_j - x_n))$$

Letting  $n = 3 \dots$

$$\bar{A} = S_{vert} + \sum_{j=1}^3 R_{ij} + \sum_{j=1}^3 L_{ij}$$

$$\begin{aligned} \bar{A} = & A_1 \tanh(B_1(x_i - x_1)) + A_2 \tanh(B_2(x_i - x_2)) + A_3 \tanh(B_3(x_i - x_3)) + \\ & A_1 \tanh(B_1(x_1 - x_n)) + A_2 \tanh(B_2(x_2 - x_n)) + A_3 \tanh(B_3(x_3 - x_n)) \end{aligned}$$

and,

$$A_1 = A_2 = A_3 = k_1$$

$$B_1 = B_2 = B_3 = k_2$$

A tanh summation method was constructed to make a manufactured solution with strong changes in slope. This ensures that the numerical approximation will not give trivial answers. then for some functions we need to impose boundary conditions. We will demonstrate how the careless implementation of a boundary condition can lead to close approximations on the interior. The speed of sound is defined with the subscript *analytic* to indicate that this is the analytical function of choice and has no physical relevance to the actual problem.

$$\tilde{A}_{analytic} = \Lambda + k_1 \tanh(k_2(\tilde{r} - \tilde{r}_{max})),$$



where,

$$\Lambda = 1 - k_1 \tanh(k_2(1 - \tilde{r}_{max})),$$

When,  $\tilde{r} = \tilde{r}_{max}$  ,  $\tilde{A}_{analytic} = 1$ . Taking the derivative with respect to  $\tilde{r}$ ,

$$\begin{aligned} \frac{\partial \tilde{A}_{analytic}}{\partial \tilde{r}} &= (1 - \tanh^2((r - r_{max})k_2)) k_1 k_2, \\ &= \frac{k_1 k_2}{\cosh^2((r - r_{max})k_2)}. \end{aligned}$$

Substitute this into the expression for  $M_\theta$  in Equation 4.1,

$$M_\theta = \sqrt{2} \sqrt{\frac{rk_1 k_2}{(\kappa - 1)(\tanh((r - r_{max})k_2)k_1 + \tanh((r_{max} - 1)k_2)k_1 + 1) \cosh^2((r - r_{max})k_2)}}$$

Now that the mean flow is defined, the integration method used to obtain the speed of sound

Initially the source terms were defined without mention of the indices of the matrices they make up. In other words, there was no fore sight on the fact that these source terms are sums of the elements within A,B, and X. To investigate the source terms in greater detail, the FORTRAN code that calls the source terms will output the terms within the source term and then sum them, instead

of just their sum. i  $[A]x = \lambda[B]x$

which can be rearranged as,

$$[A]x - \lambda[B]x = 0$$

Here,  $x$  is an eigenvector composed of the perturbation variables,  $v_r, v_\theta, v_x, p$  and  $\lambda$  is the associated eigenvalue, (Note:  $\lambda = -i\bar{\gamma}$ )

Writing this out we obtain  $\dots$ .

Linear System of Equations:

$$-i \left( \frac{k}{A} - \frac{m}{r} M_\theta \right) v_r - \frac{2}{r} M_\theta v_\theta + \frac{dp}{dr} + \frac{(\kappa - 1)}{r} M_\theta^2 p - \lambda M_x v_r = S_1 \quad (4.2)$$

Using matrix notation,

$$A_{11}x_1 - A_{12}x_2 + A_{14}x_4 - \lambda B_{11}x_1 = S_1 \quad (4.3)$$

But  $A_{14}$  and  $A_{41}$  in Kousen's paper only has the derivative operator. Since I am currently writing the matrix out term by term and not doing the matrix math to obtain the symbolic expressions, I will define  $A_{14}$  with  $dp/dr$  and  $A_{41}$  with  $dv_r/dr$ . Similarly,

$$A_{21}x_1 - A_{22}x_2 + A_{24}x_4 \quad \quad \quad -\lambda B_{22}x_2 = S_2 \quad (4.4)$$

$$A_{31}x_1 - A_{33}x_3 \quad \quad \quad -\lambda(B_{33}x_3 + B_{34}x_4) = S_3 \quad (4.5)$$

$$A_{41}x_1 + A_{42}x_2 + A_{44}x_4 \quad \quad \quad -\lambda(B_{33}x_3 + B_{44}x_4) = S_4 \quad (4.6)$$

Now we can begin looking at the source terms, term by term. They each should also converge at a known rate

## 4.4 Fairing Functions

Goal: How can we modify a manufactured solution such that the endpoints are suitable for comparison against a codes boundary condition implementation

## 4.5 Setting Boundary Condition Values Using a Fairing Function

### 4.5.1 Using $\beta$ as a scaling parameter

Defining the nondimensional radius in the same way that SWIRL does:

$$\tilde{r} = \frac{r}{r_T}$$

where  $r_T$  is the outer radius of the annulus.

The hub-to-tip ratio is defined as:

$$\sigma = \frac{r_H}{r_T} = \tilde{r}_H$$

where  $\tilde{r}_H$  is the inner radius of the annular duct. The hub-to-tip ratio can also be zero indicating the duct is hollow.

A useful and similar parameter is introduced,  $\beta$ , where  $0 \leq \beta \leq 1$

$$\beta = \frac{r - r_H}{r_T - r_H}$$

Dividing By  $r_T$

$$\begin{aligned}\beta &= \frac{\frac{r}{r_T} - \frac{r_H}{r_T}}{\frac{r_T}{r_T} - \frac{r_H}{r_T}} \\ &= \frac{\tilde{r} - \tilde{r}_H}{1 - \sigma}\end{aligned}$$

Suppose a manufactured solution  $f_{MS}$  with boundaries  $f_{MS}(r = \sigma)$  and  $f_{MS}(\tilde{r} = 1)$  is the specified analytical solution. The goal is to change the boundary conditions of the manufactured solution in such way that allows us to adequately check the boundary conditions imposed on SWIRL. Defining the manufactured solution,  $f_{MS}(\tilde{r})$ , where  $\sigma \leq \tilde{r} \leq 1$  and there are desired values of  $f$  at the boundaries desired values are going to be denoted as  $f_{minBC}$  and  $f_{maxBC}$ . The desired changes in  $f$  are defined as:

$$\begin{aligned}\Delta f_{minBC} &= f_{minBC} - f_{MS}(\tilde{r} = \sigma) \\ \Delta f_{maxBC} &= f_{maxBC} - f_{MS}(\tilde{r} = 1)\end{aligned}$$

We'd like to impose these changes smoothly on the manufactured solution function. To do this, the fairing functions,  $A_{min}(\tilde{r})$  and  $A_{max}(\tilde{r})$  where:

$$f_{BCsImposed}(\tilde{r}) = f_{MS}(\tilde{r}) + A_{min}(\tilde{r})\Delta f_{minBC} + A_{max}(\tilde{r})\Delta f_{maxBC}$$

Then, in order to set the condition at the appropriate boundary, the following conditions are set,

$$A_{min}(\tilde{r} = \sigma) = 1$$

$$A_{min}(\tilde{r} = 1) = 0$$

$$A_{max}(\tilde{r} = 1) = 1$$

$$A_{max}(\tilde{r} = \sigma) = 0$$

If  $A_{min}(\tilde{r})$  is defined as a function of  $A_{max}(\tilde{r})$  then only  $A_{max}(\tilde{r})$  needs to be defined, therefore

$$A_{min}(\tilde{r}) = 1 - A_{max}(\tilde{r})$$

It is also desirable to set the derivatives for the fairing function at the boundaries incase there are boundary conditions imposed on the derivatives of the fairing function.

$$\frac{\partial A_{max}}{\partial \tilde{r}}|_{\tilde{r}=\sigma} = 0$$

$$\frac{\partial A_{max}}{\partial \tilde{r}}|_{\tilde{r}=1} = 0$$

$$\frac{\partial A_{min}}{\partial \tilde{r}}|_{\tilde{r}=\sigma} = 0$$

$$\frac{\partial A_{min}}{\partial \tilde{r}}|_{\tilde{r}=1} = 0$$

### 4.5.2 Minimum Boundary Fairing Function

Looking at  $A_{min}$  first, the polynomial is:

$$A_{min}(\beta) = a + b\beta + c\beta^2 + d\beta^3$$

$$A_{min}(\tilde{r}) = a + b\left(\frac{\tilde{r} - \sigma}{1 - \sigma}\right) + c\left(\frac{\tilde{r} - \sigma}{1 - \sigma}\right)^2 + d\left(\frac{\tilde{r} - \sigma}{1 - \sigma}\right)^3$$

Taking the derivative,

$$A'_{min}(\tilde{r}) = b\left(\frac{1}{1 - \sigma}\right) + 2c\left(\frac{1}{1 - \sigma}\right)\left(\frac{\tilde{r} - \sigma}{1 - \sigma}\right) + 3d\left(\frac{1}{1 - \sigma}\right)\left(\frac{\tilde{r} - \sigma}{1 - \sigma}\right)^2$$

$$A'_{min}(\beta) = \left(\frac{1}{1 - \sigma}\right)[b + 2c\beta + 3d\beta^2]$$

Now we will use the conditons mentioned earlier as constraints to this system of equations Using the possible values of  $\tilde{r}$ ,

$$A_{min}(\sigma) = a \quad \quad \quad = 1$$

$$A_{min}(1) = a + b + c + d \quad \quad \quad = 0$$

$$A'_{min}(\sigma) = b \quad \quad \quad = 0$$

$$A'_{min}(1) = b + 2c + 3d \quad \quad \quad = 0$$

which has the solution,

$$a = 1$$

$$b = 0$$

$$c = -3$$

$$d = 2$$

giving the polynomial as:

$$A_{min}(\tilde{r}) = 1 - 3 \left( \frac{\tilde{r} - \sigma}{1 - \sigma} \right)^2 + 2 \left( \frac{\tilde{r} - \sigma}{1 - \sigma} \right)^3$$

### 4.5.3 Max boundary polynomial

Following the same procedure for  $A_{max}$  gives

$$A_{min}(\tilde{r}) = 3 \left( \frac{\tilde{r} - \sigma}{1 - \sigma} \right)^2 - 2 \left( \frac{\tilde{r} - \sigma}{1 - \sigma} \right)^3$$

### 4.5.4 Corrected function

The corrected function is then,

$$\begin{aligned} f_{BCsImposed}(\tilde{r}) &= f_{MS}(\tilde{r}) + A_{min}\Delta f_{minBC} + A_{max}\Delta f_{maxBC} \\ &= f_{MS}(\tilde{r}) + \left( 1 - 3 \left( \frac{\tilde{r} - \sigma}{1 - \sigma} \right)^2 + 2 \left( \frac{\tilde{r} - \sigma}{1 - \sigma} \right)^3 \right) [\Delta f_{minBC}] \\ &\quad + \left( 3 \left( \frac{\tilde{r} - \sigma}{1 - \sigma} \right)^2 - 2 \left( \frac{\tilde{r} - \sigma}{1 - \sigma} \right)^3 \right) [\Delta f_{maxBC}] \\ f_{BCsImposed}(\beta) &= f_{MS}(\beta) + \Delta f_{minBC} + (3\beta^2 - 2\beta^3) [\Delta f_{maxBC} - \Delta f_{minBC}] \end{aligned}$$

Note that we're carrying the correction throughout the domain, as opposed to limiting the correction at a certain distance away from the boundary. The application of this correction ensures that there is no discontinuous derivatives inside the domain; as suggested in Roach's MMS guidelines (insert ref)

What is meant by "just because  $A_{min}$  and its first derivative go to zero doesn't mean that the second derivatives"

#### 4.5.5 Symbolic Sanity Checks

We want to ensure that  $f_{BCsImposed}$  has the desired boundary conditions,  $f_{minBC/maxBC}$  instead of the original boundary values that come along for the ride in the manufactured solutions,  $f_{MS}(\tilde{r} = \sigma/1)$ . In another iteration of this method, we will be changing the derivative values, so let's check the values of  $\frac{\partial f_{BCsImposed}}{\partial \tilde{r}}$  to make sure those aren't effected unintentionally.

##### Symbolic Sanity Check 1

The modified manufactured solution,  $f_{BCsImposed}$  with the fairing functions  $A_{min}$  and  $A_{max}$  substituted in is,

$$f_{BCsImposed}(\tilde{r}) = \left( 3 \left( \frac{\tilde{r} - \sigma}{1 - \sigma} \right)^2 - 2 \left( \frac{\tilde{r} - \sigma}{1 - \sigma} \right)^3 \right) [\Delta f_{maxBC}].$$

Further simplification yields,

$$\begin{aligned} f_{BCsImposed}(\tilde{r} = \sigma) &= \left( f_{MS}(\tilde{r} = \sigma) + \Delta f_{minBC} + \left( 3 \left( \frac{\sigma - \sigma}{1 - \sigma} \right)^2 - 2 \left( \frac{\sigma - \sigma}{1 - \sigma} \right)^3 \right) [\Delta f_{maxBC} - \Delta f_{minBC}] \right) \\ &= f_{MS}(\tilde{r} = \sigma) + \Delta f_{minBC} \\ &= f_{MS}(\tilde{r} = \sigma) + (f_{minBC} - f_{MS}(\tilde{r} = \sigma)) \\ &= f_{minBC} \end{aligned}$$



$$\begin{aligned}
f_{BCsImposed}(\tilde{r} = 1) &= \left( f_{MS}(\tilde{r} = 1) + \Delta f_{minBC} + \left( 3 \left( \frac{1-\sigma}{1-\sigma} \right)^2 - 2 \left( \frac{1-\sigma}{1-\sigma} \right)^3 - \right) [\Delta f_{maxBC} - \Delta f_{minBC}] \right) \\
&= f_{MS}(\tilde{r} = 1) + \Delta f_{maxBC} \\
&= f_{MS}(\tilde{r} = 1) + (f_{maxBC} - f_{MS}(\tilde{r} = 1)) \\
&= f_{maxBC}
\end{aligned}$$

$$\begin{aligned}
&\frac{\partial}{\partial \tilde{r}} \left( f_{BCsImposed}(\tilde{r}) = \left( 3 \left( \frac{\tilde{r}-\sigma}{1-\sigma} \right)^2 - 2 \left( \frac{\tilde{r}-\sigma}{1-\sigma} \right)^3 \right) [\Delta f_{maxBC}] \right) \\
&\frac{\partial f_{MS}}{\partial \tilde{r}} + \left( \frac{6}{1-\sigma} \right) \left( \left( \frac{\tilde{r}-\sigma}{1-\sigma} \right) - \left( \frac{\tilde{r}-\sigma}{1-\sigma} \right)^2 \right) (\Delta f_{maxBC} - \Delta f_{minBC})
\end{aligned}$$

At  $\tilde{r} = \sigma$ , the derivative is:

$$\begin{aligned}
&\frac{\partial f_{MS}}{\partial \tilde{r}}|_{\sigma} \\
&\frac{\partial f_{MS}}{\partial \tilde{r}}|_1
\end{aligned}$$

#### 4.5.6 Min boundary derivative polynomial

The polynomial is of the form:

$$\begin{aligned}
B_{min}(\beta) &= a + b\beta + c\beta^2 + d\beta^3 \\
B_{min}(\tilde{r}) &= a + b \left( \frac{\tilde{r}-\sigma}{1-\sigma} \right) + c \left( \frac{\tilde{r}-\sigma}{1-\sigma} \right)^2 + d \left( \frac{\tilde{r}-\sigma}{1-\sigma} \right)^3
\end{aligned}$$

Taking the derivative,

$$B'_{min}(\tilde{r}) = b \left( \frac{1}{1-\sigma} \right) + 2c \left( \frac{1}{1-\sigma} \right) \left( \frac{\tilde{r}-\sigma}{1-\sigma} \right) + 3d \left( \frac{1}{1-\sigma} \right) \left( \frac{\tilde{r}-\sigma}{1-\sigma} \right)^2$$

$$B'_{min}(\beta) = \left( \frac{1}{1-\sigma} \right) [b + 2c\beta + 3d\beta^2]$$

Applying the four constraints gives:

$$a = 0$$

$$b = (1 - \sigma)$$

$$a + b + c + d = 0$$

$$2 + 2c + 3d = 0$$

$$c + d = -b$$

$$2c + 3d = -b$$

$$c = -2b$$

$$d = b$$

and the min boundary derivative polynomial is:

$$B_{min}(\tilde{r}) = b \left( \frac{\tilde{r}-\sigma}{1-\sigma} \right) - 2b \left( \frac{\tilde{r}-\sigma}{1-\sigma} \right)^2 + b \left( \frac{\tilde{r}-\sigma}{1-\sigma} \right)^3$$

$$= (1 - \sigma) \left( \left( \frac{\tilde{r}-\sigma}{1-\sigma} \right) - 2 \left( \frac{\tilde{r}-\sigma}{1-\sigma} \right)^2 + \left( \frac{\tilde{r}-\sigma}{1-\sigma} \right)^3 \right)$$

#### 4.5.7 Polynomial function, max boundary derivative

The polynomial is of the form:

The polynomial is of the form:

$$B_{max}(\beta) = a + b\beta + c\beta^2 + d\beta^3$$

$$B_{max}(\tilde{r}) = a + b\left(\frac{\tilde{r} - \sigma}{1 - \sigma}\right) + c\left(\frac{\tilde{r} - \sigma}{1 - \sigma}\right)^2 + d\left(\frac{\tilde{r} - \sigma}{1 - \sigma}\right)^3$$

which has the derivative,

$$B'_{max}(\tilde{r}) = b\left(\frac{1}{1 - \sigma}\right) + 2c\left(\frac{1}{1 - \sigma}\right)\left(\frac{\tilde{r} - \sigma}{1 - \sigma}\right) + 3d\left(\frac{1}{1 - \sigma}\right)\left(\frac{\tilde{r} - \sigma}{1 - \sigma}\right)^2$$

$$B'_{max}(\beta) = \left(\frac{1}{1 - \sigma}\right)[b + 2c\beta + 3d\beta^2]$$

Applying the four constraints gives:

$$a = 0$$

$$b = 0$$

$$a + b + c + d = 0$$

$$b + 2c + 3d = (1 - \sigma)$$

working this out:

$$c + d = 0$$

$$2c + 3d = (1 - \sigma)$$

gives

$$c = -(1 - \sigma) d = (1 - \sigma)$$

and the max boundary derivative polynomial is:

$$B_{max}(\tilde{r}) = (1 - \sigma) \left( - \left( \frac{\tilde{r} - \sigma}{1 - \sigma} \right)^2 + \left( \frac{\tilde{r} - \sigma}{1 - \sigma} \right)^3 \right)$$

#### 4.5.8 Putting it together

The corrected function is then:

$$\begin{aligned} f_{BCsImposed}(\tilde{r}) &= f_{MS} + B_{min}(\tilde{r}) \Delta f'_{minBC} + B_{max}(\tilde{r}) \Delta f'_{maxBC} \\ &= f_{MS} + \\ &\quad (1 - \sigma) \left( \left( \frac{\tilde{r} - \sigma}{1 - \sigma} \right) - \left( \frac{\tilde{r} - \sigma}{1 - \sigma} \right)^2 \right) \Delta f'_{minBC} + \\ &\quad (1 - \sigma) \left( - \left( \frac{\tilde{r} - \sigma}{1 - \sigma} \right)^2 + \left( \frac{\tilde{r} - \sigma}{1 - \sigma} \right)^3 \right) (\Delta f'_{minBC} + \Delta f'_{maxBC}) \end{aligned}$$

# Chapter 5

## Results and Discussion

### 5.1 Verification

### 5.2 Introduction

The goal of this chapter is to document the observed order of accuracy and the grid convergence index (GCI) for various validation and verification test cases.

#### 5.2.1 Statement of the received results and their analysis

The convergence rates for the two numerical approximation techniques used in SWIRL will be presented for a set of test cases using MMS/MES.

for the

### 5.3 Code Verificaton using the Method of Manufactured Solutions

Figure 5-1 shows the manufactured solution for the mean flow profile. The tangent summation method (TSM) was used to generate the axial mach number and for the speed of sound. The tangential mach number was then numerically approximated by

using the composite trapezoidal rule. The manufactured mean flow profile is unique in that it has been generated solely for the verification of SWIRL and does not have physical significance. The “kinks” in the solution will allow there to be a significant magnitude for the derivatives of these solution.

The TSM was also used to generate the manufactured solutions for the perturbation variables in Figures 5-2-5-5. The boundary condition values of the MS for  $\bar{v}_r$ ,  $dP/dr$  must reflect the actual boundary conditions in SWIRL. This is set by using a fairing function. Note that the hard wall condition requires  $\bar{v}_r$  to be zero which is shown in Figure 5-2. While the boundaries for the pressure perturbation may not be known, the boundary condition is set with the derivative of the pressure perturbation, which may or may not be zero depending if there is liner for the test case. This is why these functions no longer resemble tangent function, but in essence still are.

The results from the numerical integration is presented in Figure 5-6. Although the slope of the line appears linear, the TSM was still used to generate the MS for the speed of sound. To demonstrate the effect of using denser grids, the difference between the expected speed of sound to the actual speed of sound is shown in Figure 5-8 as a function of radius (needs label). Note that the error does not reach machine precision for the first grid and approaches zero as more grid points are used.

As the error decreases, it will decrease at a known rate depending on the numerical integration scheme used. Since the composite trapezoidal rule has an order of accuracy of 2, it is expected that the approximated order of accuracy will approach two as the error approaches zero. This behavior is shown in Figure 5-14 where the approximated line is the  $L2_{norm}$  of the speed of sound error. The slope ( i.e. the asymptotic rate of convergence ) approached two for numerical integration as the grid spacing decreases (See Figure 5-15) .

For the LEE, a second and fourth order central differencing scheme is used for the approximated radial derivatives and then compared to the source terms generated for

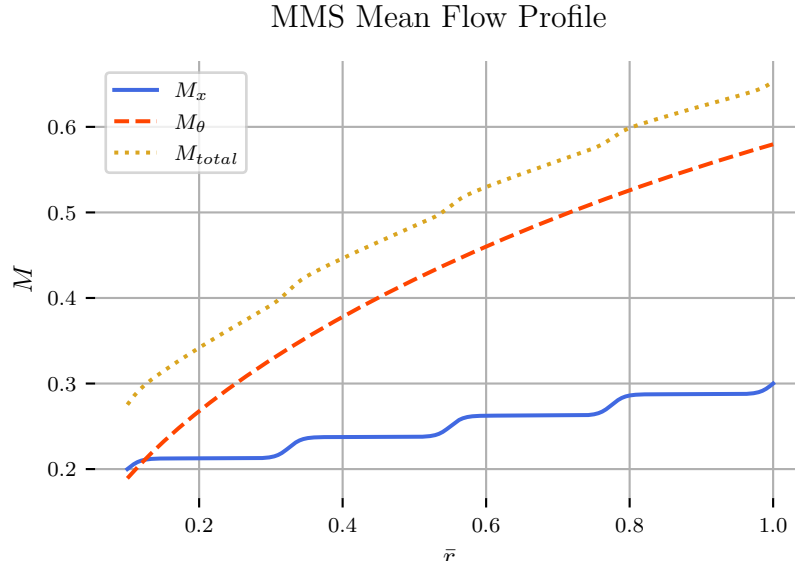


Figure 5-1: The manufactured mean flow test case using a summation of Tangents for  $A$  and  $M_x$

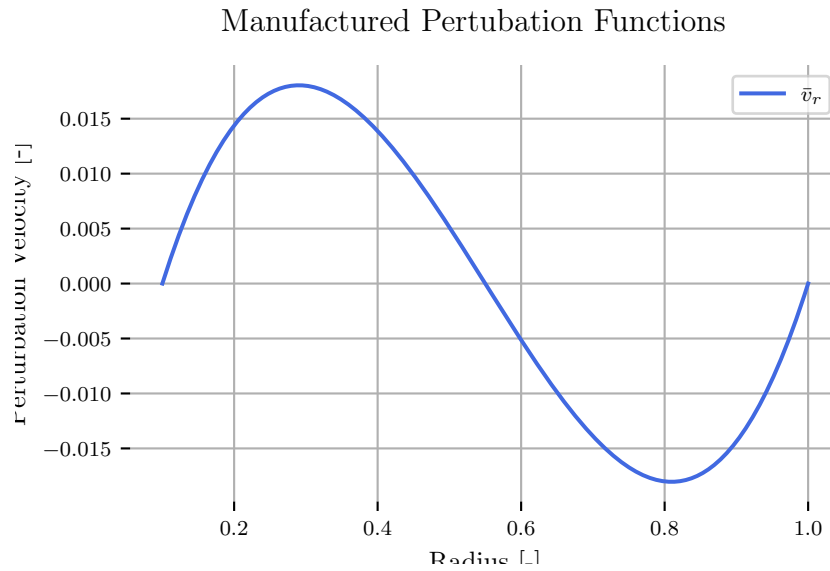


Figure 5-2: The manufactured perturbation functions  $\bar{v}_r$

the MMS in Figure 5-9. (Discuss Error here...skeptical on the plot...5-13)

The  $L2_{norm}$  and the asymptotic rate of convergence is shown for the two differencing schemes in 5-15 and 5-16. (How should is dicuss this?)

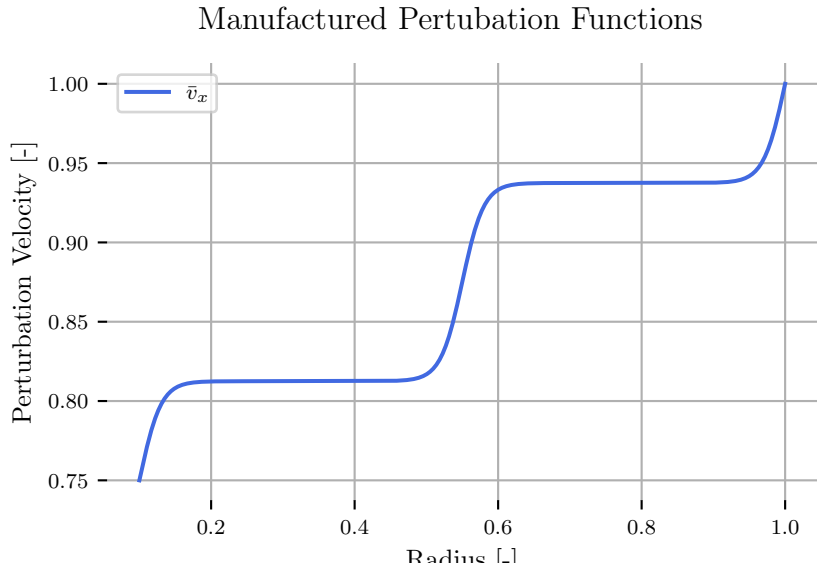


Figure 5-3: The manufactured perturbation functions , $v_x$

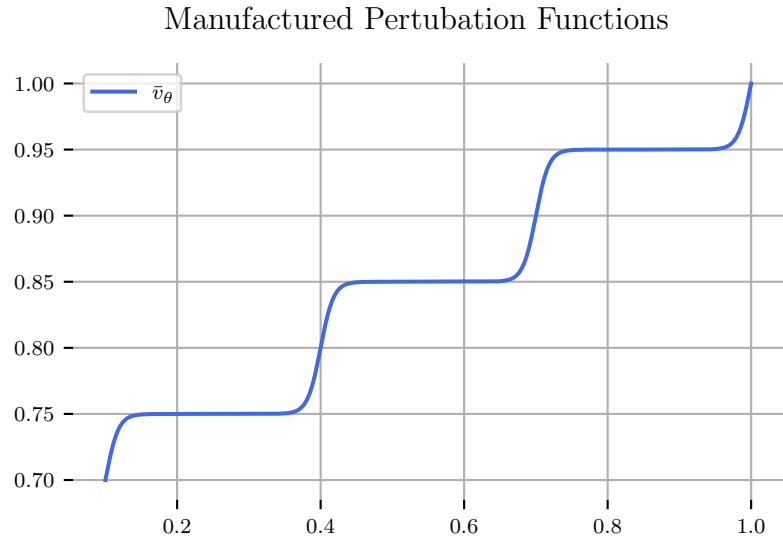


Figure 5-4: The manufactured perturbation functions , $v_\theta$



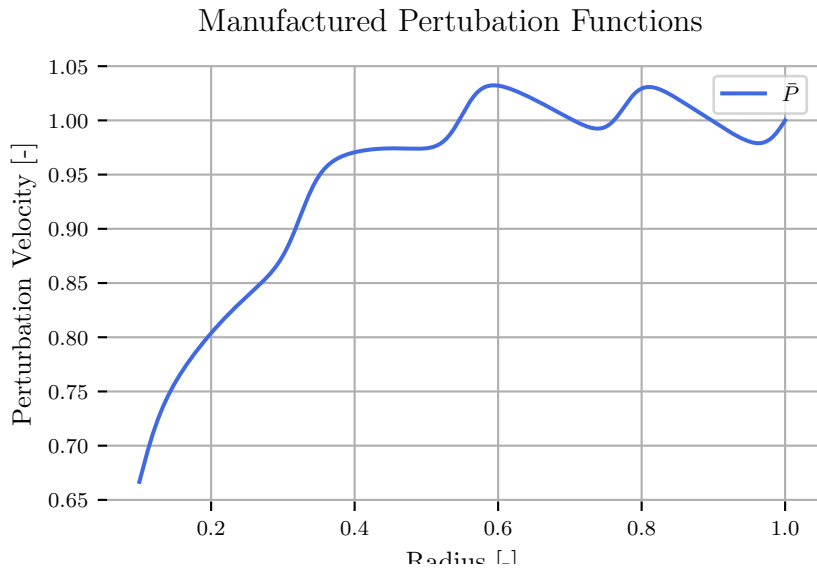


Figure 5-5: The manufactured perturbation functions,  $\bar{P}$

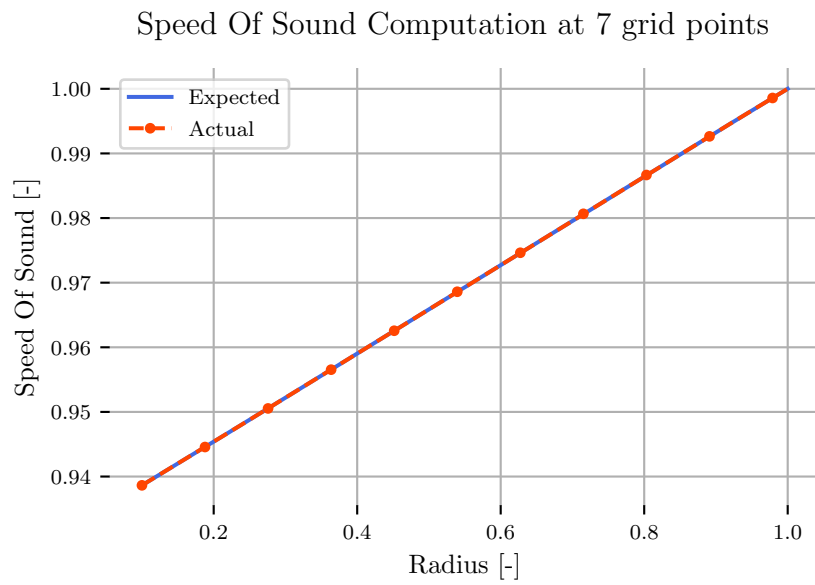


Figure 5-6: A comparison of the speed of sound, expected vs actual at the lowest grid to show similarities in solution

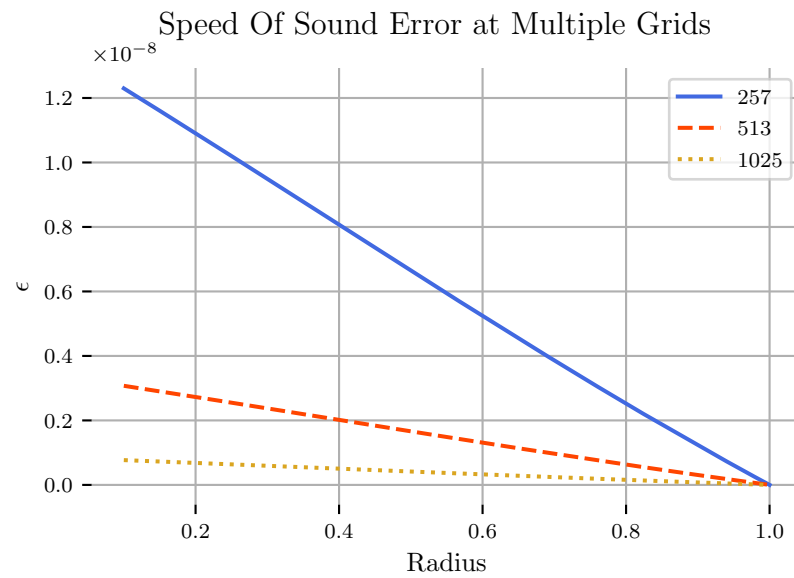


Figure 5-7: A comparison of the speed of sound error at three grid

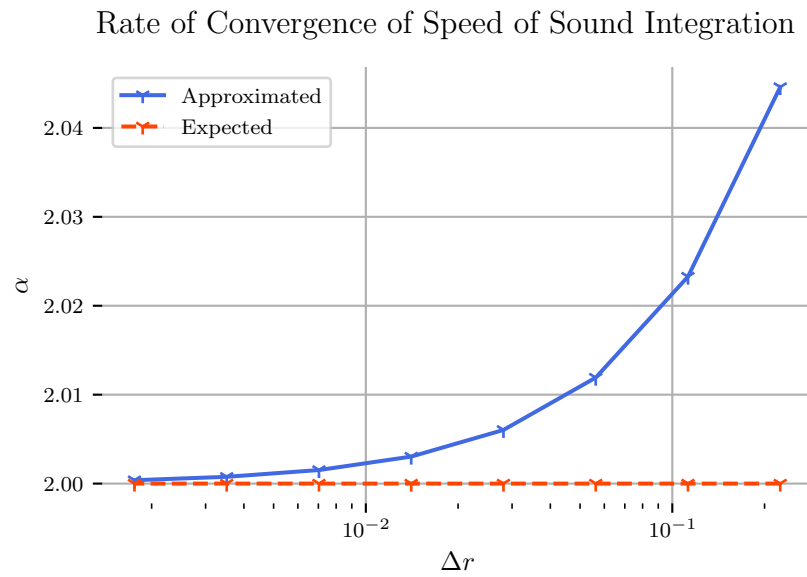


Figure 5-8: A comparison of the speed of sound error at three grid

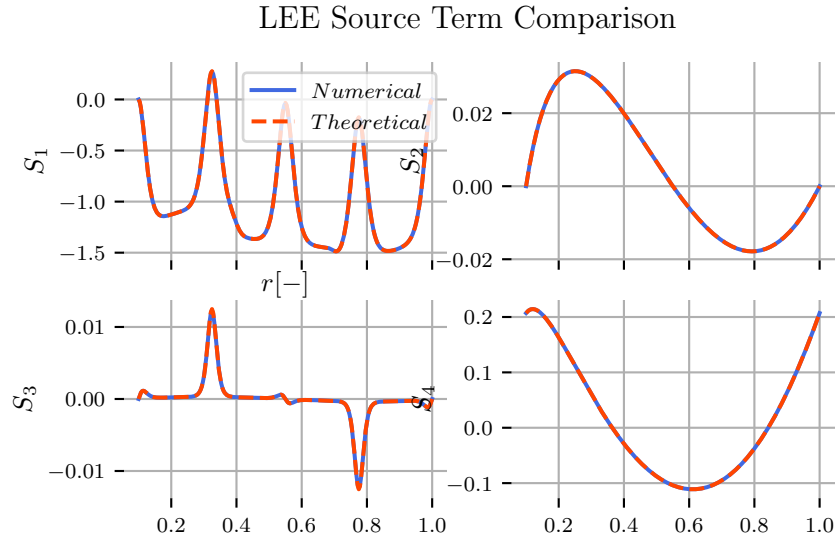


Figure 5-9: LEE Source Terms

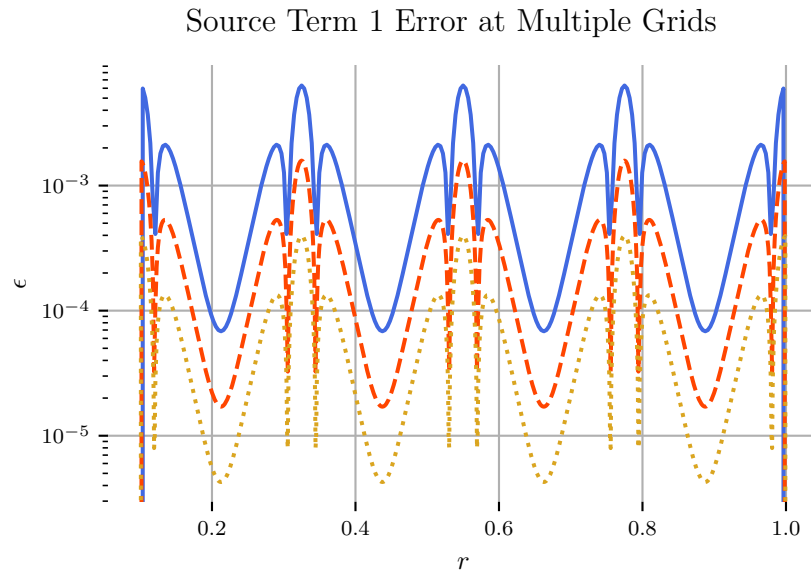


Figure 5-10: LEE Source Term Error

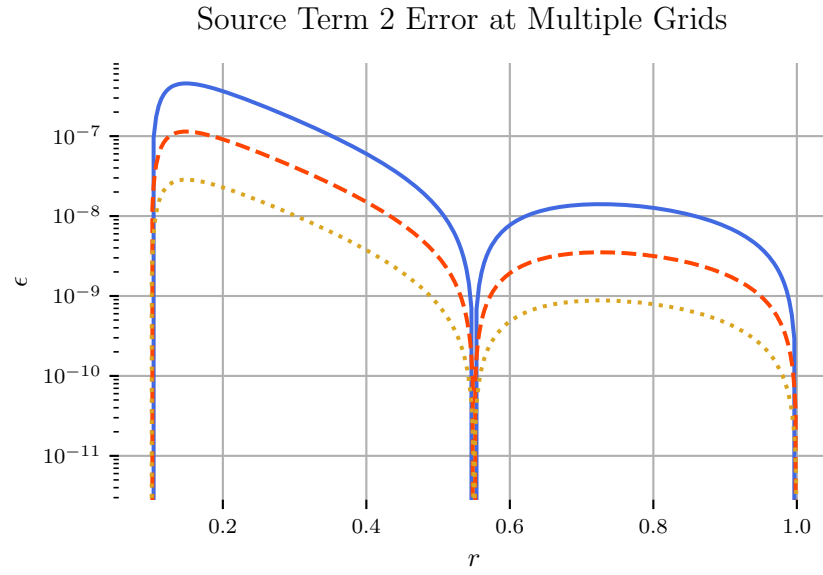


Figure 5-11: LEE Source Term Error

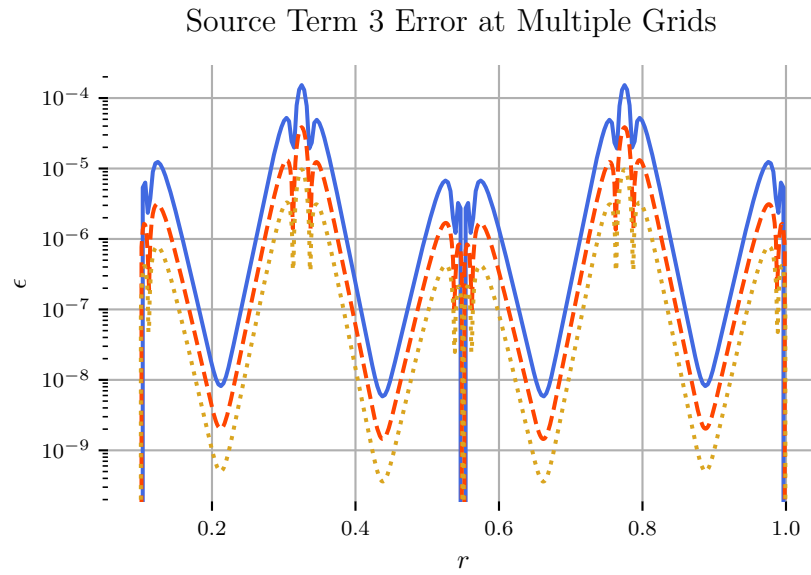


Figure 5-12: LEE Source Term Error

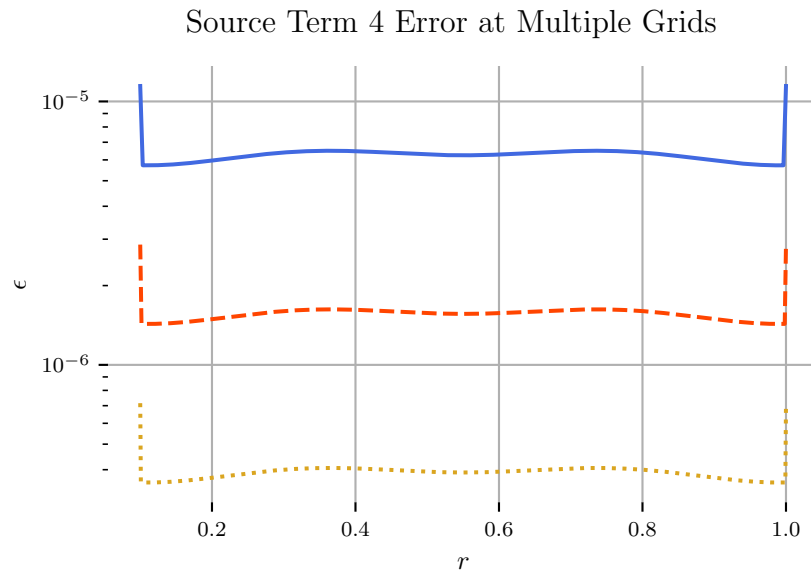


Figure 5-13: LEE Source Term Error

Log-log plot of the  $L2_{norm}$  from the Speed of Sound Integration

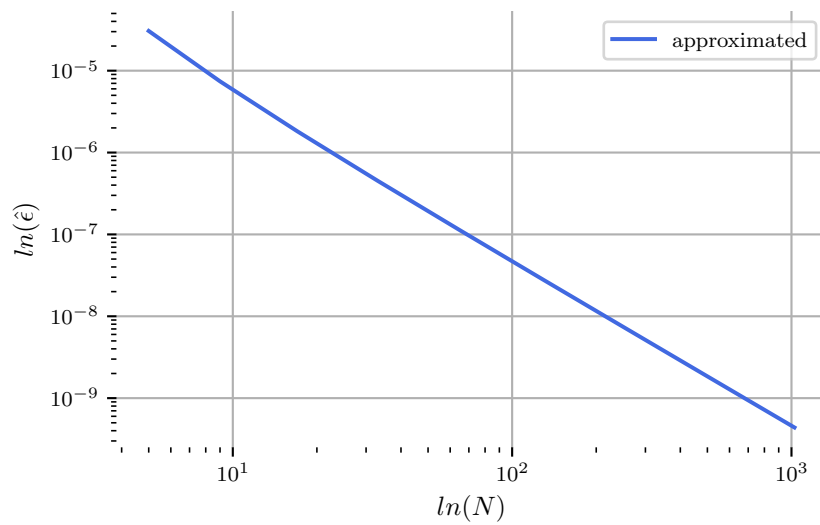


Figure 5-14: L2 Norm comparison for the speed of sound integration for the compound trapezoidal rule

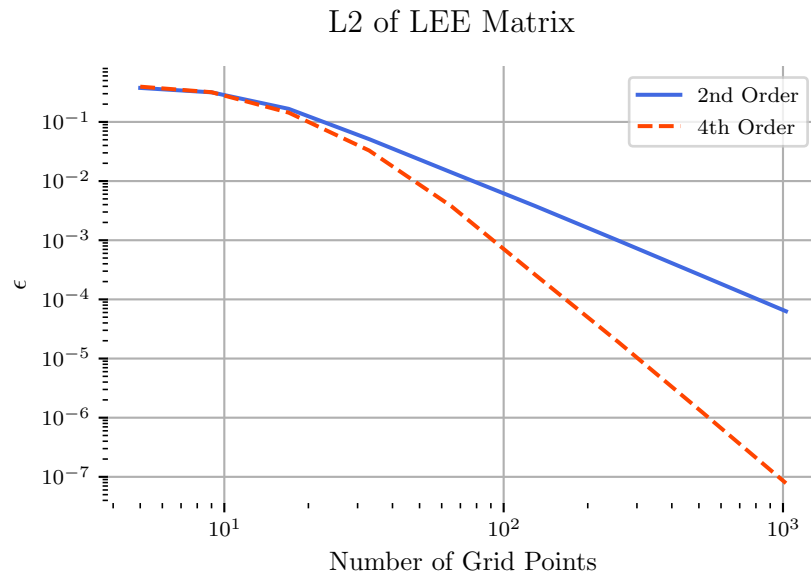


Figure 5-15: ROC for the speed of sound integration for the compound trapezoidal rule

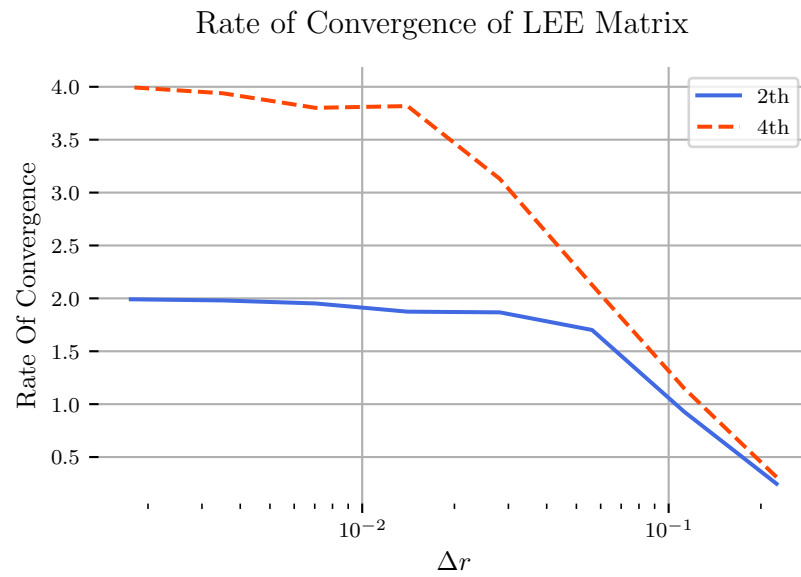


Figure 5-16: ROC for the LEE using second and fourth order central differencing for the radial derivative

### 5.3.0.1 Test Case 1

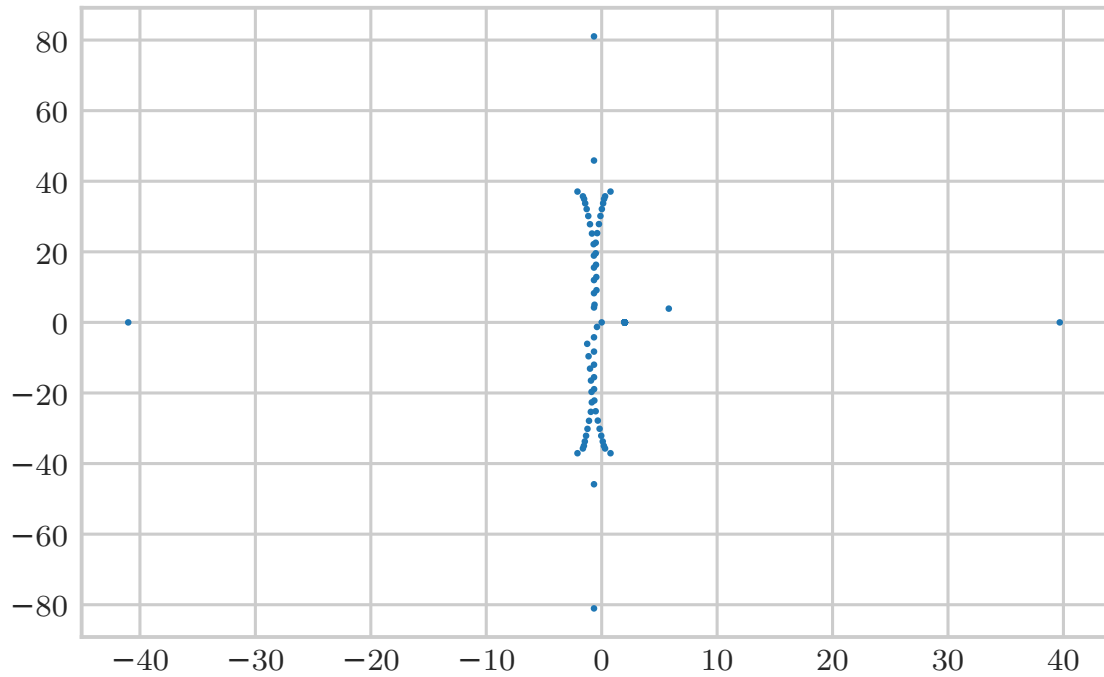
A comparison was conducted for a hollow cylinder undergoing uniform flow with acoustic liners along the outer duct perimeter. The azimuthal mode number, reduced frequency, mach number and duct liner admittance is reported below,

$$m = 2$$

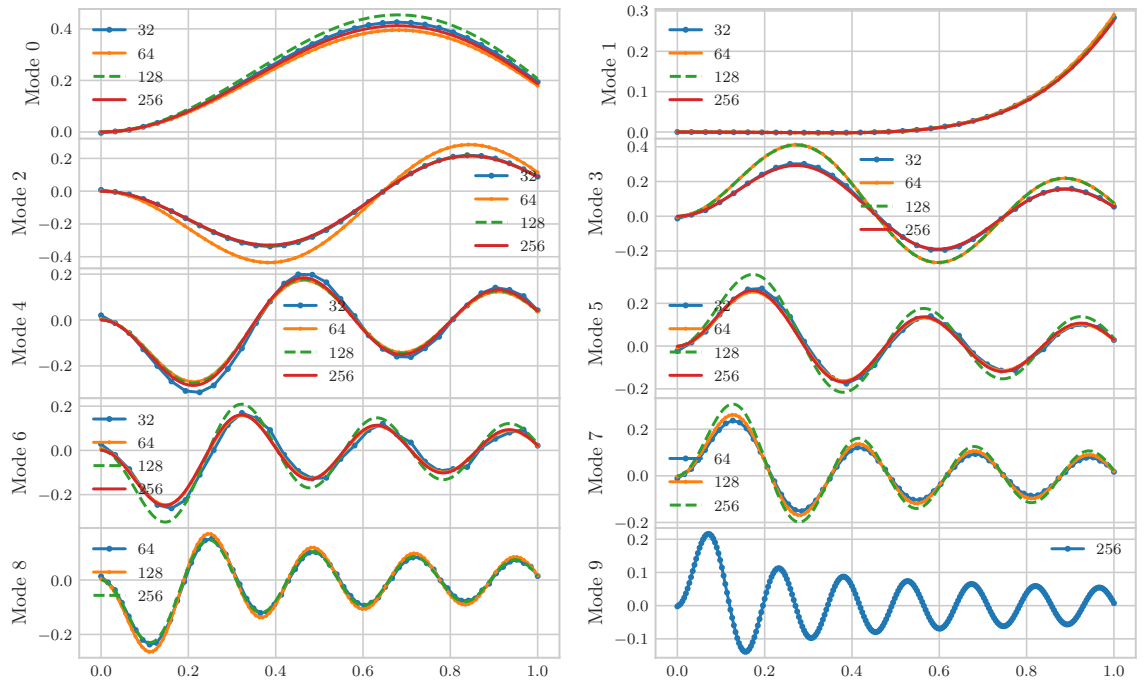
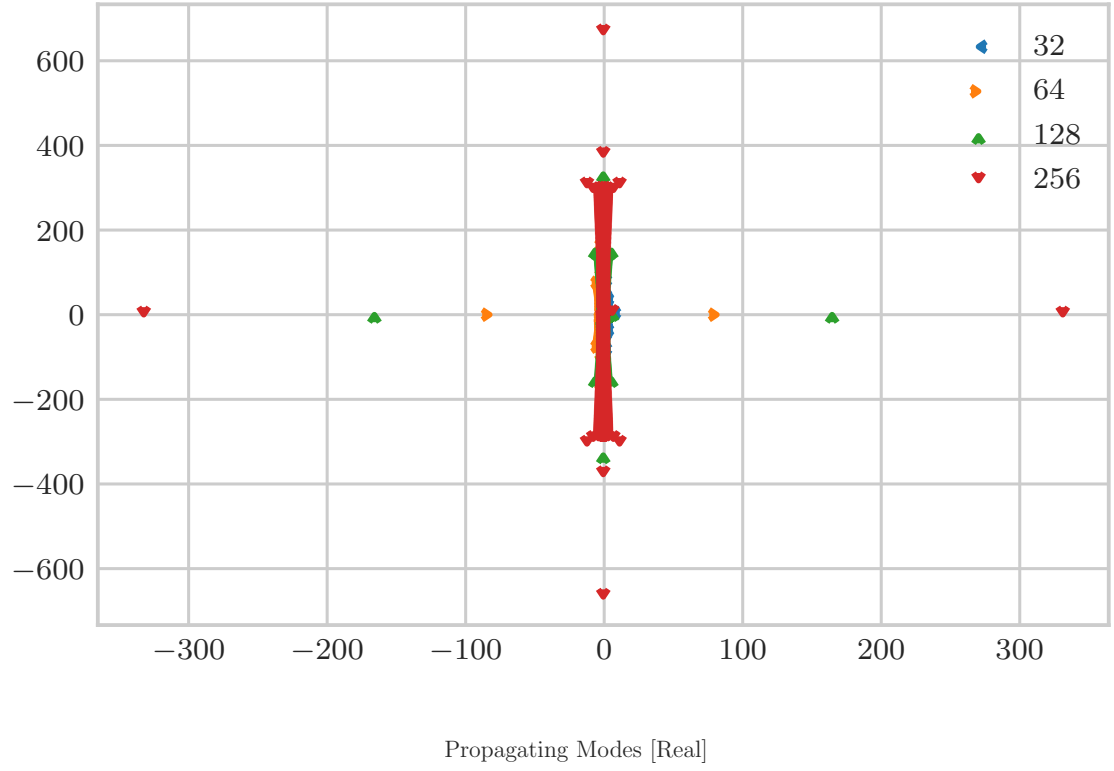
$$k = \frac{\omega r_T}{A_T} = -1$$

$$M_x = 0.5$$

$$\eta_T = 0.72 + 0.42i$$

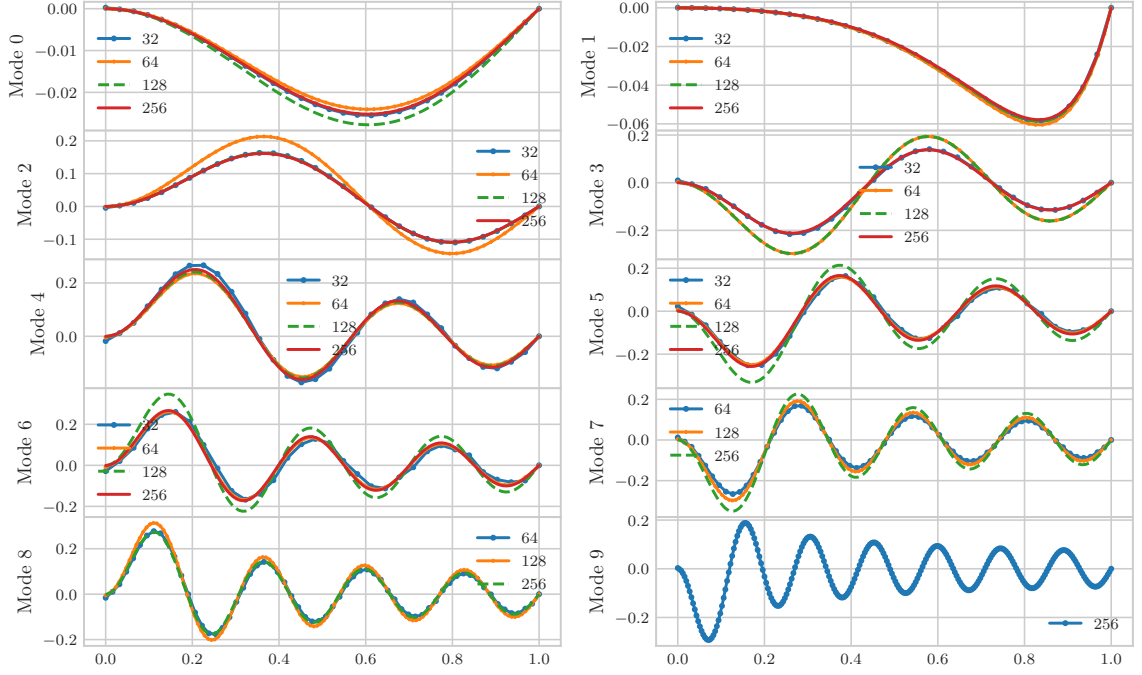


The results shown in 5.1 are in moderately good agreement. The results were obtained by visually comparing the output in `gam.acc` for 32 grid points. Note that the indices for the SWIRL deliverable are different that the ones obtained for the most





### Propagating Modes [Imaginary]

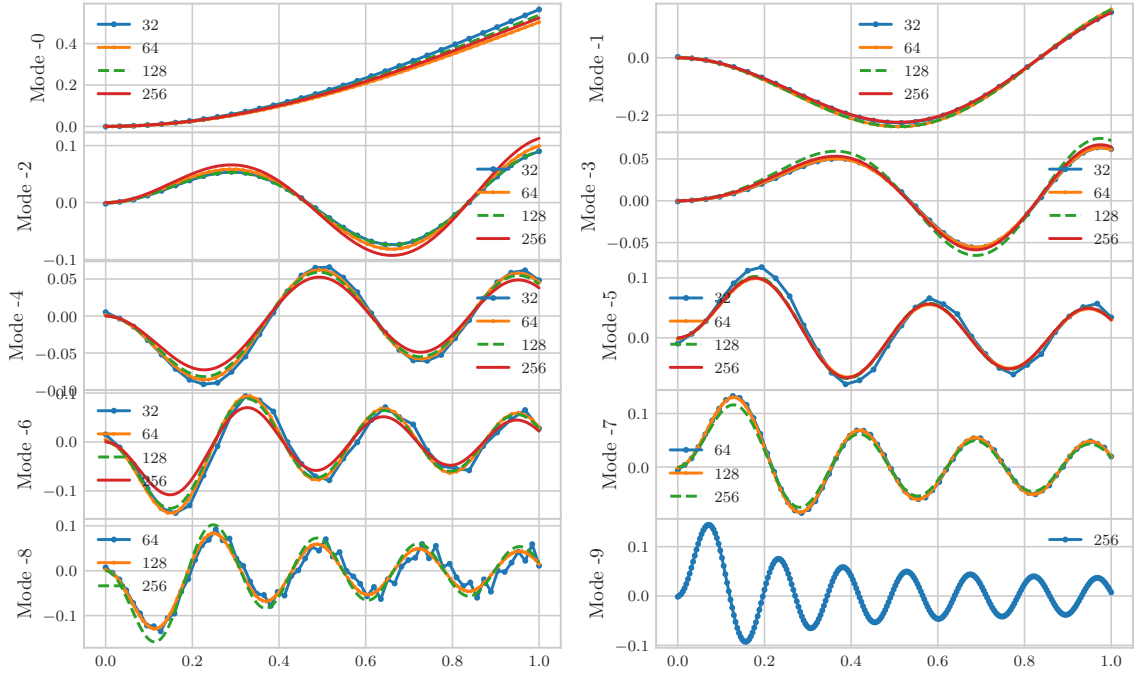


recent version of the code. While the convective axial wavenumbers show agreement to machine precision, this is not particularly insightful given that there are an infinite number of possible solutions that could satisfy the eigenvalue problem. The results that are of concern are propagating modes that are not convecting with the mean flow. The scatter plot of the axial wavenumbers show some sporadic behaviour around the imaginary axis. The results from the MMS along with this plot indicate that more grid points are going to be needed if a finite difference technique is to be used.

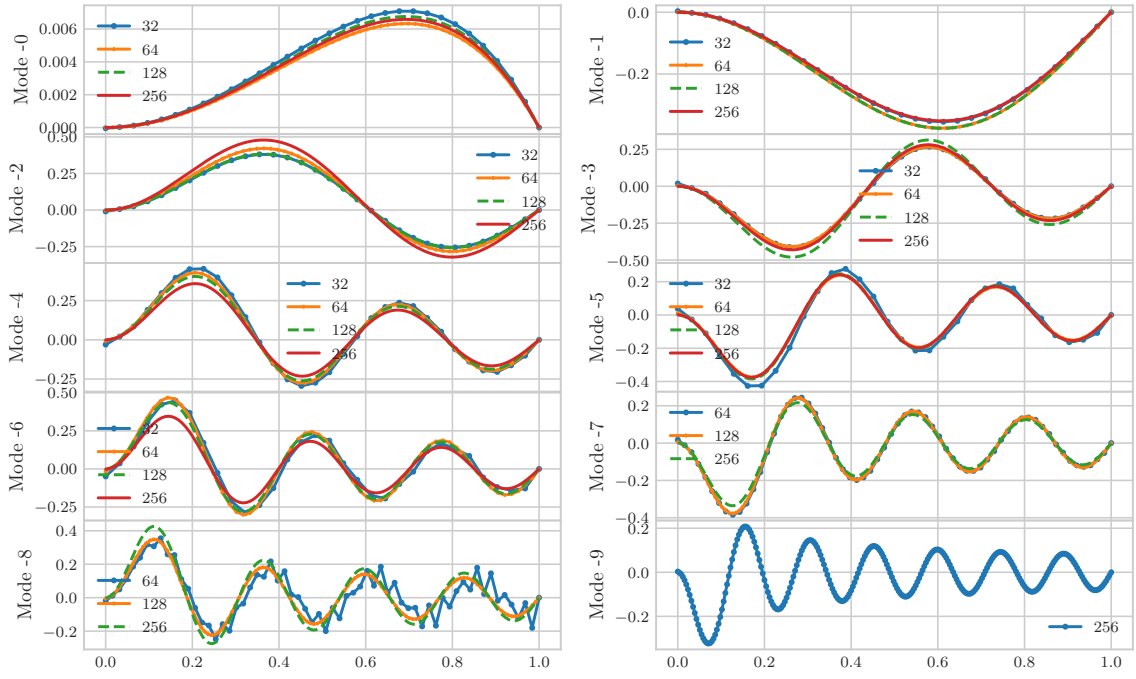
The first 10 propagating and decaying modes are plotted in 5.3.0.1-5.3.0.1.

-

Decaying Modes [Real]



Decaying Modes [Imaginary]



$\gamma_n^\pm$	Kousen Ref. [15]	Kousen report	srcF2008	index	current	index
$\gamma_0^+$	$0.620 - 5.014i$	$0.6195 - 5.0139i$	$0.61954 - 5.01386i$	60	$0.620755853112 - 5.00592416941i$	34
$\gamma_1^+$	$-5.820 - 3.897i$	$-5.8195 - 3.8968i$	$-5.81953 - 3.89677i$	58	$-0.581267772517 - 3.90050864568i$	33
$\gamma_2^+$	$0.445 - 9.187i$	$0.4453 - 9.1868i$	$0.44533 - 9.18684i$	59	$0.451569491142 - 9.12191317214i$	31
$\gamma_3^+$	$0.453 - 13.062i$	$0.4539 - 13.062i$	$0.45389 - 13.0615i$	57	$0.464247902898 - 12.8487472519i$	29
$\gamma_4^+$	$0.480 - 16.822i$	$0.4795 - 16.822i$	$0.47952 - 16.8216i$	55	$0.492340380223 - 16.3292825150i$	27
$\gamma_5^+$	$0.503 - 20.531i$	$0.5029 - 20.531i$	$0.50287 - 20.5307i$	51	$0.514522630594 - 19.5817182568i$	25
$\gamma_6^+$	$0.522 - 24.213i$	$0.5220 - 24.213i$	$0.52202 - 24.2129i$	50	$0.516658239854 - 22.5715880605i$	23
$\gamma_7^+$	$0.538 - 27.880i$	$0.5376 - 27.880i$	$0.53754 - 27.8800i$	48	-	-
$\gamma_8^+$	$0.550 - 31.537i$	$0.5502 - 31.537i$	$0.55024 - 31.5368i$	47	-	-
$\gamma_9^+$	$0.589 - 49.75i$	$0.5891 - 49.754i$	$0.58745 - 49.7669i$	33	-	-
$\gamma_0^-$	$0.410 + 1.290i$	$0.4101 + 1.2904i$	$0.41009 + 1.29037i$	64	$0.409973310292 + 1.29020083859i$	64
$\gamma_1^-$	$1.259 + 6.085i$	$1.2595 + 6.0852i$	$1.25949 + 6.08517i$	63	$1.25530612217 + 6.07214375548i$	62
$\gamma_2^-$	$1.146 + 9.668i$	$1.1457 + 9.6679i$	$1.14567 + 9.66787i$	62	$1.13696444935 + 9.59622801724i$	60
$\gamma_3^-$	$1.022 + 13.315i$	$1.0218 + 13.315i$	$1.02183 + 13.3150i$	61	$1.00950576515 + 13.0957277529i$	58
$\gamma_4^-$	$0.943 + 16.977i$	$0.9425 + 16.977i$	$0.94250 + 16.9767i$	56	$0.928059983039 + 16.4791343118i$	56
$\gamma_5^-$	$0.891 + 20.635i$	$0.8908 + 20.635i$	$0.89075 + 20.6353i$	54	$0.856678172769 + 22.6544943903i$	52
$\gamma_6^-$	$0.855 + 24.288i$	$0.8549 + 24.288i$	$0.85490 + 24.2883i$	53	$0.941762848775 + 25.3460188358i$	50
$\gamma_7^-$	$0.829 + 27.937i$	$0.8288 + 27.937i$	$0.82877 + 27.9369i$	52	-	-
$\gamma_8^-$	$0.809 + 31.581i$	$0.8089 + 31.581i$	$0.80891 + 31.5812i$	49	-	-
$\gamma_9^-$	$0.755 + 49.77i$	$0.7547 + 49.772i$	$0.75658 + 49.7851i$	39	-	-

Table 5.1: Table 4.3 data

# References

- [1] Michael JT Smith. Aircraft noise. *Cambridge Aerospace Series*, 1989.
- [2] Mathias Basner, Charlotte Clark, Anna Hansell, James I Hileman, Sabine Janssen, Kevin Shepherd, and Victor Sparrow. Aviation noise impacts: State of the science. pages 41–50, 2017.
- [3] Covid19 pandemic observations on the ongoing recovery of the aviation industry accessible version united states government accountability office, 2021.
- [4] Department Of Transportation Federal Aviation Administration. Aviation environmental and energy policy statement - july 2012, 2012.
- [5] *INDEPENDENT EXPERT INTEGRATED TECHNOLOGY GOALS ASSESSMENT AND REVIEW FOR ENGINES AND AIRCRAFT REPORT*. 2019.
- [6] Aircraft geared architecture reduces fuel cost and noise, 2015.
- [7] Konrad Kozaczuk. Engine nacelles design – problems and challenges. *Proceedings of the Institution of Mechanical Engineers, Part G: Journal of Aerospace Engineering*, 231:2259–2265, 10 2017.
- [8] VV Golubev and HM Atassi. Sound propagation in an annular duct with mean potential swirling flow. *Journal of Sound and Vibration*, 198(5):601–616, 1996.
- [9] J. L. Kerrebrock. Small disturbances in turbomachine annuli with swirl. <https://doi.org/10.2514/3.7370>, 15:794–803, 5 2012.

- [10] J. L. KERREBROCK. Waves and wakes in turbomachine annuli with swirl. 1974.
- [11] Edmane Envia, Alexander G. Wilson, and Dennis L. Huff. Fan noise: A challenge to caa, 8 2004.
- [12] A. J. COOPER and N. PEAKE. Propagation of unsteady disturbances in a slowly varying duct with mean swirling flow. *Journal of Fluid Mechanics*, 445:207–234, 10 2001.
- [13] M. E. Goldstein. Characteristics of the unsteady motion on transversely sheared mean flows. *Journal of Fluid Mechanics*, 84:305, 1 1978.
- [14] M. E. Goldstein. Scattering and distortion of the unsteady motion on transversely sheared mean flows. *Journal of Fluid Mechanics*, 91:601–632, 1979.
- [15] A. KAPUR and P. MUNGUR. Sound interaction with a helical flow contained in an annular duct with radial gradients of flow, density and temperature. 1973.
- [16] A. L.P. Maldonado, R. J. Astley, J. Coupland, G. Gabard, and D. Sutliff. Sound propagation in lined annular ducts with mean swirling flow. American Institute of Aeronautics and Astronautics Inc, AIAA, 2016.
- [17] Kenneth Kousen. Pressure modes in ducted flows with swirl. In *Aeroacoustics Conference*, page 1679, 1996.
- [18] Kenneth A Kousen. Eigenmode analysis of ducted flows with radially dependent axial and swirl components. In *CEAS/AIAA Joint Aeroacoustics Conference, 1st, Munich, Germany*, pages 1085–1094, 1995.
- [19] V. V. Golubev and H. M. Atassi. Acoustic-vorticity waves in swirling flows. *Journal of Sound and Vibration*, 209:203–222, 1 1998.

- [20] Vladimir V. Golubev and Hafiz M. Atassi. Acoustic-vorticity modes in an annular duct with mean vortical swirling flow. *3rd AIAA/CEAS Aeroacoustics Conference*, pages 804–814, 1997.
- [21] Christopher K.W. Tam and Laurent Auriault. The wave modes in ducted swirling flows. *Journal of Fluid Mechanics*, 371:1–20, 9 1998.
- [22] Ronald Nijboer. Eigenvalues and eigenfunctions of ducted swirling flows. *7th AIAA/CEAS Aeroacoustics Conference and Exhibit*, 2001.
- [23] Ying Guan, Kai H. Luo, and Tong Q. Wang. Sound transmission in a lined annular duct with mean swirling flow. *American Society of Mechanical Engineers, Noise Control and Acoustics Division (Publication) NCAD*, pages 135–144, 6 2009.
- [24] A. J. Cooper. Effect of mean entropy on unsteady disturbance propagation in a slowly varying duct with mean swirling flow. *Journal of Sound and Vibration*, 291:779–801, 4 2006.
- [25] H. Posson and N. Peake. The acoustic analogy in an annular duct with swirling mean flow. *Journal of Fluid Mechanics*, 726:439–475, 2013.
- [26] C. J. Heaton and N. Peake. Algebraic and exponential instability of inviscid swirling flow. *Journal of Fluid Mechanics*, 565:279–318, 10 2006.
- [27] Ray Hixon, Adrian Sescu, and Vasanth Allampalli. Towards the prediction of noise from realistic rotor wake/stator interaction using caa. volume 6, pages 203–213. Elsevier Ltd, 2010.
- [28] R. YURKOVICH. Attenuation of acoustic modes in circular and annular ducts in the presence of sheared flow. *13th Aerospace Sciences Meeting*, 1 1975.

- [29] J. M. Tyler and T. G. Sofrin. Axial flow compressor noise studies. *SAE Technical Papers*, 1 1962.
- [30] Small-amplitude disturbances in turbomachine flows with swirl - david w. wundrow - google books.
- [31] K. M. Case. Stability of inviscid plane couette flow. *The Physics of Fluids*, 3:143, 11 2004.
- [32] P N Shankar. Acoustic refraction and attenuation in cylindrical and annular ducts, 1972.
- [33] P. T. Vo and W. Eversman. A method of weighted residuals with trigonometric basis functions for sound transmission in circular ducts. *Journal of Sound and Vibration*, 56:243–250, 1 1978.
- [34] R. J. Astley and W. Eversman. A finite element formulation of the eigenvalue problem in lined ducts with flow. *Journal of Sound and Vibration*, 65:61–74, 7 1979.
- [35] Christopher J. Roy. Review of code and solution verification procedures for computational simulation. *Journal of Computational Physics*, 205:131–156, 5 2005.
- [36] Kambiz Salari and Patrick Knupp. Code verification by the method of manufactured solutions, 2000.
- [37] Jack L. Kerrebrock. *Aircraft engines and gas turbines*. MIT Press, 1992.
- [38] N. K. Agarwal and M. K. Bull. Acoustic wave propagation in a pipe with fully developed turbulent flow. *Journal of Sound and Vibration*, 132:275–298, 7 1989.